Available online at www.sciencedirect.com
ScienceDirect
Journal of Organometallic Chemistry 693 (2008) 933–946
Journal of Organometallic Chemistry
www.elsevier.com/locate/jorganchem

Heterotrimetallic and heterotetrametallic transition metal complexes

Rico Packheiser, Petra Ecorchard, Bernhard Walfort, Heinrich Lang *

Technische Universität Chemnitz, Fakultät für Naturwissenschaften, Institut für Chemie, Lehrstuhl für Anorganische Chemie, Straße der Nationen 62, 09111 Chemnitz, Germany

Received 1 October 2007; received in revised form 22 November 2007; accepted 28 November 2007
Available online 4 December 2007

Abstract

The synthesis of the ruthenium σ-acetylides (η^5-C_5H_5)L_2Ru–C≡C–bipy (**4a**, L = PPh_3; **4b**, L_2 = dppf; bipy = 2,2′-bipyridine-5-yl; dppf = 1,1′-bis(diphenylphosphino)ferrocene) is possible by the reaction of [(η^5-C_5H_5)L_2RuCl] (**1**) with 5-ethynyl-2,2′-bipyridine (**2a**) in the presence of NH_4PF_6 followed by deprotonation with DBU. Heterobimetallic Fc–C≡C–NCN–Pt–C≡C–R (**10a**, R = bipy; **10b**, R = C_5H_4N-4; Fc = (η^5-C_5H_5)(η^5-C_5H_4)Fe; NCN = [1,4-$C_6H_2(CH_2NMe_2)_2$-2,6]$^-$) is accessible by the metathesis of Fc–C≡C–NCN–PtCl (**9**) with lithium acetylides LiC≡C–R (**2a**, R = bipy; **2b**, R = C_5H_4N-4).The complexation behavior of **4a** and **4b** was investigated.Treatment of these molecules with [$MnBr(CO)_5$] (**13**) and {[Ti](μ–σ,π-C≡C$SiMe_3$)$_2$}MX (**15a**, MX = Cu(N≡CMe)PF_6; **15b**, MX = Cu(N≡CMe)BF_4; **16**, MX = $AgOClO_3$; [Ti] = (η^5-$C_5H_4SiMe_3$)$_2$Ti), respectively, gave the heteromultimetallic transition metal complexes (η^5- C_5H_5)L_2Ru–C≡C–bipy[$Mn(CO)_3Br$] (**14a**: L = PPh_3; **14b**: L_2 = dppf) and [(η^5-C_5H_5)L_2Ru–C≡C–bipy{[Ti](μ–σ,π-C≡C$SiMe_3$)$_2$}M]X (**17a**: L = PPh_3, M = Cu, X = BF_4; **17b**: L_2 = dppf, M = Cu, X = PF_6; **18a**: L = PPh_3, M = Ag, X = ClO_4; **18b**: L_2 = dppf, M = Ag, X = ClO_4) in which the appropriate transition metals are bridged by carbon-rich connectivities.

The solid-state structures of **4b**, **10b**, **12** and **17b** are reported. The main structural feature of **10b** is the square-planar-surrounded platinum(II) ion and its linear arrangement. In complex **12** the N-atom of the pendant pyridine unit coordinates to a [*mer*,*trans*-(*NN′N*)$RuCl_2$] (*NN′N* = 2,6-bis-[(dimethylamino)methyl]pyridine) complex fragment, resulting in a distorted octahedral environment at the Ru(II) centre. In **4b** a 1,1′-bis(diphenylphosphino)ferrocene building block is coordinated to a cyclopentadienylruthenium-σ-acetylide fragment. Heterotetrametallic **17b** contains a (η^5-C_5H_5)(dppf)Ru–C≡C–bipy unit, the bipyridine entity of which is chelate-bonded to [{[Ti](μ–σ,π-C≡C$SiMe_3$)$_2$}Cu]$^+$. Within this arrangement copper(I) is tetra-coordinated and hence, possesses a pseudo-tetrahedral coordination sphere.

The electrochemical behavior of **4**, **10b**, **12**, **17** and **18** is discussed. As typical for these molecules, reversible oxidation processes are found for the iron(II) and ruthenium(II) ions. The attachment of copper(I) or silver(I) building blocks at the bipyridine moiety as given in complexes **17** and **18** complicates the oxidation of ruthenium and consequently the reduction of the group-11 metals is made more difficult, indicating an interaction over the organic bridging units.

The above described complexes add to the so far only less investigated class of compounds of heteromultimetallic carbon-rich transition metal compounds.

Keywords: Ruthenium; Platinum; Copper; Silver; Acetylide; Ferrocene

1. Introduction

The covalent and dative linkage of metal complex fragments to generate heteromultimetallic transition metal complexes, a hitherto scarcely explored class of compounds, is an important theme within contemporary organometallic chemistry [1]. One approach to verify this subject is given by using the concept of molecular "Tinkertoys", which was independently established by Michl and Stoddart [2,3]. Individually functionalized multitopic inorganic, organic, organometallic and/or metal-organic molecules can be considered as modular building blocks and can

* Corresponding author. Tel.: +49 371 531 21210; fax: +49 371 531 21219.
E-mail address: heinrich.lang@chemie.tu-chemnitz.de (H. Lang).

0022-328X/$ - see front matter © 2007 Elsevier B.V. All rights reserved.
doi:10.1016/j.jorganchem.2007.11.052

successfully be assembled to a specific building design to give complexes of higher nuclearity with novel structures. Such molecules may show unique and often unusual properties.

In context with this background, we focus here on the use of alkynyl-functionalized ferrocenes, bis(alkynyl) titanocenes, NCN pincer molecules (NCN = [4-X–$C_6H_2(CH_2NMe_2)_2$-2,6]$^-$; X = C≡C, ...), and alkynyl-substituted pyridine ligands as building blocks in the synthesis of heterotri- and heterotetrametallic systems in which the appropriate transition metals are connected by carbon-rich bridging units.

2. Results and discussion

2.1. Synthesis and characterization

The synthesis of two new mono- and heterobimetallic rutheniumacetylide complexes with a pendant 2,2′-bipyridine-5-yl unit (=bipy) can be realized as shown in Scheme 1. Addition of 5-ethynyl-2,2′-bipyridine (**2a**) to the ruthenium(II) complex [(η^5-C_5H_5)L_2RuCl] (**1a**, L = PPh_3; **1b**, L_2 = dppf (dppf = 1,1′-bis(diphenylphosphino)ferrocene)) in the presence of NH_4PF_6 in a 1:1 mixture of dichloromethane and methanol resulted in the formation of yellow (η^5-C_5H_5)L_2Ru–C≡C–bipy (**4a**, L = PPh_3; **1b**, L_2 = dppf). Within the reaction of terminal alkynes with coordinatively unsaturated metal complexes, metal vinylidene transition metal species (**3a**, **3b**, Scheme 1) are ubiquitous formed as intermediates [4]. When **1** is treated with the terminal alkyne **2a**, due to the intrinsic basicity of the bipyridine moiety, a somewhat different behavior is observed as compared with those of regular terminal alkynes. Next to the expected ruthenium vinylidene [(η^5-C_5H_5)L_2Ru=C=C(H)(bipy)]$^+$ (**3a**) also the σ-acetylide complex [(η^5-C_5H_5)L_2Ru–C≡C–bipyH]$^+$ (**3b**) with a pendant pyridinium unit was produced (Scheme 1), as evidenced by the appearance of two $^{31}P\{^1H\}$ NMR resonance signals as well as a $\nu_{C\equiv C}$ and $\nu_{C=C}$ vibration in the IR spectra. It is most likely that a vinylidene complex is formed as the primary product, which is then converted to a pyridinium system [5]. Removal of the vinylidene β-hydrogen atom or the bipyridine-bonded proton by methoxide or DBU (DBU = 1,8-diazabicyclo[5.4.0]undec-7-ene) caused the formation of the ruthenium σ-acetylides **4a** and **4b** containing a pendant 2,2′-bipyridine-5-yl entity, which is capable of coordinating to different transition metal fragments and consequently is suitable for the construction of transition metal complexes of higher nuclearity.

Another molecule with a multitopic ligand allowing to introduce further metal-containing building blocks is Fc–C≡C–NCN–Pt–C≡C–R (**10a**, R = bipy; **10b**, R = C_5H_4N-4; Fc = (η^5-C_5H_5)(η^5-C_5H_4)Fe; NCN = [$C_6H_2(CH_2NMe_2)_2$-2,6]$^-$). The preparation of this molecule is shown in Scheme 2 and includes several consecutive steps.

Heterobimetallic Fc–C≡C–NCN–Pt–C≡C–R (**10a**, R = bipy; **10b**, R = C_5H_4N-4) is accessible by a consecutive synthesis methodology including carbon–carbon cross-coupling, lithiation, *trans*-metallation, and metathesis reactions. Following the Sonogashira cross-coupling protocol [6], Fc–C≡C–NCNH (**7**) (NCNH = 1-$C_6H_3(CH_2NMe_2)_2$-3,5) was prepared by reacting ethynylferrocene (**5**) with I-1-$C_6H_3(CH_2NMe_2)_2$-3,5 (**6**) in the presence of [$(Ph_3P)_2PdCl_2$/CuI] and diisopropylamine as solvent [7]. A possibility to introduce a platinum chloride entity into NCN pincer molecules is given by a lithiation–*trans*-metallation procedure: lithiation of **7** with ^{n}BuLi and subsequent treatment of the respective lithium salt with [$(Et_2S)_2PtCl_2$] (**8**) produced heterobimetallic Fc–C≡C–NCN–PtCl (**9**) [7], which further reacted with in-situ lithiated HC≡C–R (**2a**, R = bipy; **2b**, R = C_5H_4N-4) to give the title complexes **10a** and **10b**, respectively (Scheme 2). However, compound **10a** was always obtained together with small amounts of unreacted **9**, even when **Li–2a** was used in a

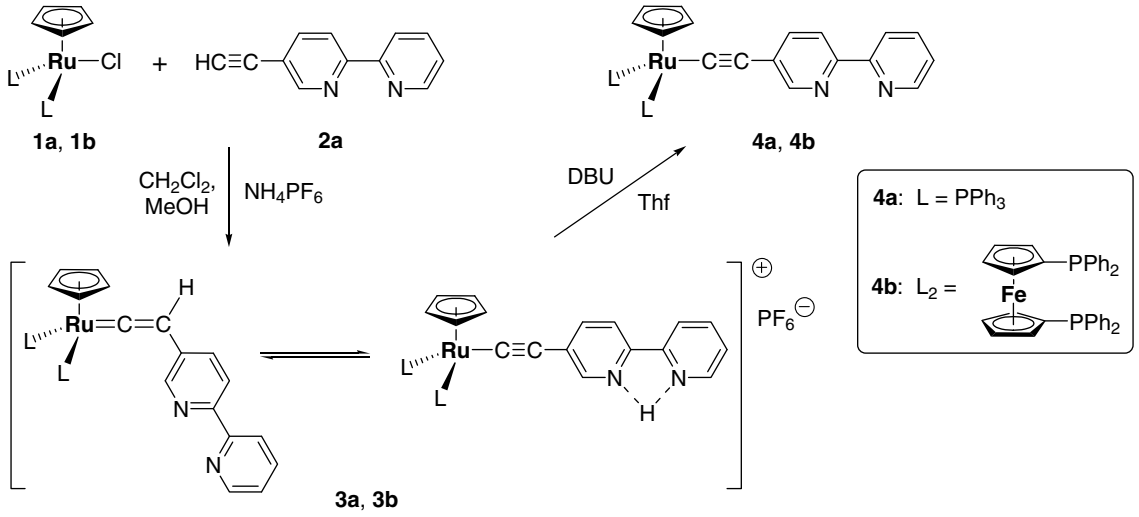

Scheme 1. Synthesis of **4a** and **4b** from **1a**, **1b** and **2a** by the intermediate formation of **3a** and **3b**, respectively.

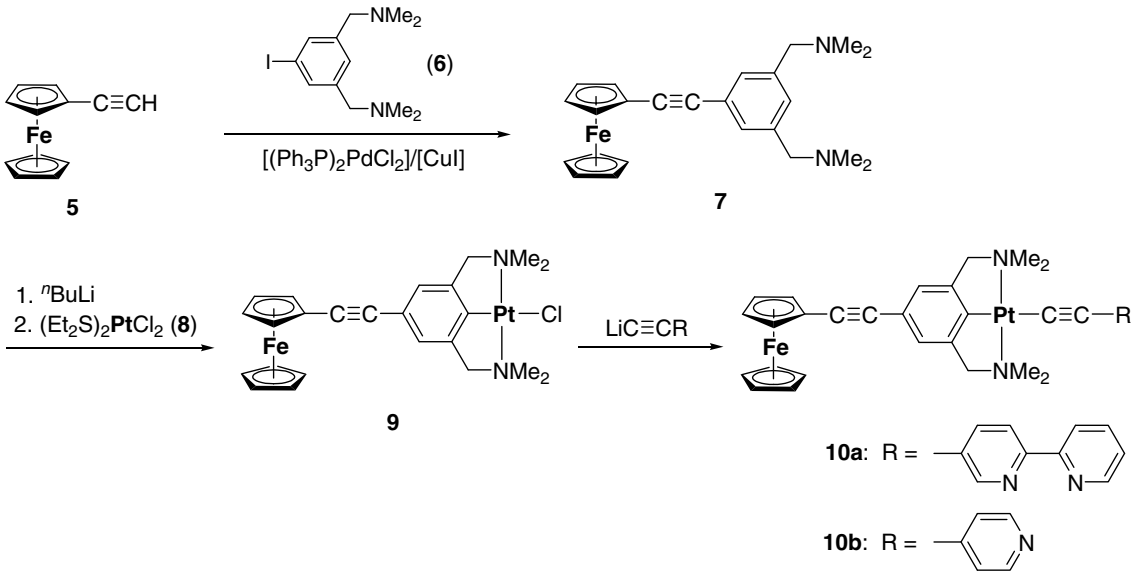

Scheme 2. Preparation of the heterobimetallic Fe–Pt complexes **10a** and **10b**.

twofold excess. Because a separation of **10a** from **9** was not possible, no further reactions were carried out with this compound.

When **10b** was reacted with the dinitrogen-bridged diruthenium complex [Ru]N≡N[Ru] (**11**) ([Ru] = [η^3-*mer*-{2,6-(Me_2NCH_2)$_2$$C_5H_3N$}$RuCl_2$]) [8], the formation of neutral heterotrimetallic **12** occured by the liberation of N_2 (Eq. (1)). The reaction could be followed visually by the change of the color of the reaction solution from yellow to intense red.

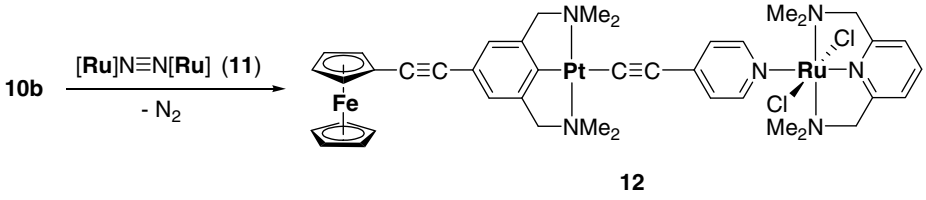

(1)

Complexes **4a** and **4b** possess with their terminal bipyridine unit a further N-ligating site which should allow to successfully introduce further transition metal entities.

Thus, these compounds were reacted with [$MnBr(CO)_5$] (**13**) and the heterobimetallic organometallic π-tweezer {[Ti](μ–σ,π-C≡$CSiMe_3$)$_2$}MX (**15a**, MX = Cu(N≡C-Me)PF_6; **15b**, MX = Cu(N≡CMe)BF_4; **16**, MX = AgO-ClO_3; [Ti] = (η^5-$C_5H_4SiMe_3$)$_2$Ti) in ethanol (synthesis of **14a**, **14b**) or tetrahydrofuran (synthesis of **17** and **18**), whereby the CO and acetonitrile ligands in **13** and **15** were replaced by the bidenate donor 2,2′-bipyridine (Scheme 3). The appropriate reactions resulted in a color change from yellow to red. After appropriate work-up, complexes **14**, **17** and **18** could be isolated in good yield as orange-red solids (Section 4). They are soluble in, for example, dichloromethane, chloroform and tetrahydrofuran. Solutions containing these molecules are somewhat sensitive to oxygen and moisture, especially those containing the monodentate triphenylphosphine ligands at ruthenium.

In the newly synthesized complexes **10**, **12**, **14**, **17** and **18** different transition metal atoms such as titanium, manganese, ruthenium, iron, platinum and copper are brought in close proximity to each other by carbon-rich bridging units.

Complexes **4**, **10**, **12**, **14**, **17** and **18** were fully characterized by elemental analysis, IR- and NMR spectroscopy (^{1}H, ^{13}C{^{1}H}, ^{31}P{^{1}H}), while **10a**, **10b** and **12** were further characterized by mass spectrometry. Complexes **4b**, **10b** and **17b** were additionally subjected to single crystal X-ray structure determination.

Most characteristic in the IR spectra of **4**, **14**, **17** and **18** is the appearance of a sharp absorption band which can be assigned to the ruthenium-bonded acetylide unit. For **4a** and **4b** this $\nu_{C\equiv C}$ vibration is found at ca. 2070 cm^{-1}, while in complexes **14**, **17** and **18** in which the bipyridine unit coordinates to $MnBr(CO)_3$ and [{[Ti](μ–σ,π-C≡$CSiMe_3$)$_2$}M]$^+$, respectively, this band is shifted by 30 cm^{-1} to lower wavenumbers. This points to a weaker carbon–carbon triple bond and is typical for similar compounds in which nitrogen-containing ligands are coordinated to a ML_n transition metal fragment or are protonated, *i.e.* (η^5-C_5H_5)$(PPh_3)_2$Ru–C≡C–C_5H_4N-[$W(CO)_5$] [5]. Further

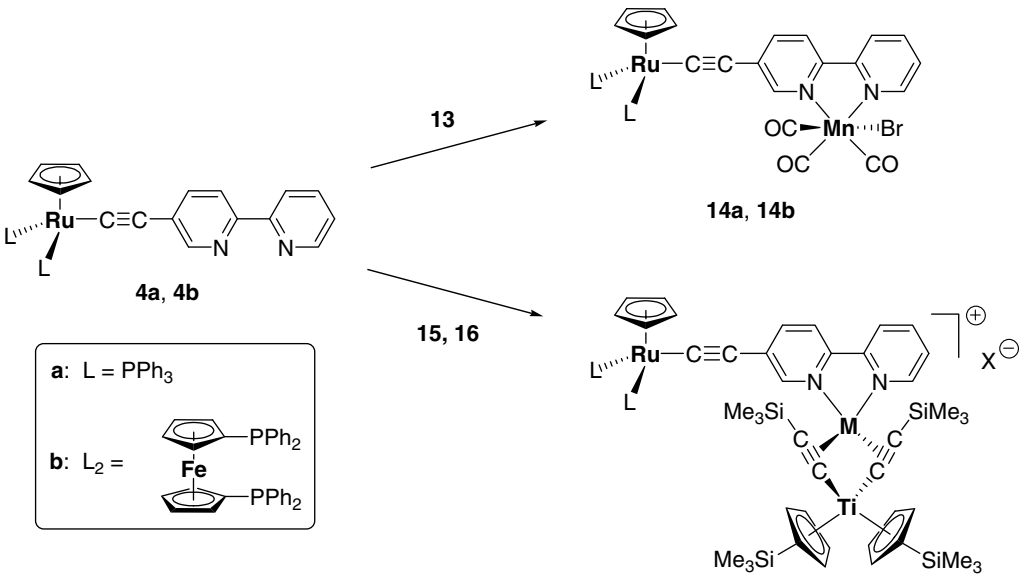

Scheme 3. Synthesis of heterotri- and heterotetrametallic **14**, **17** and **18**.

representative bands which can be observed are the carbonyl vibrations in **14** and the $\nu_{C\equiv C}$ band for the Ti–C≡C unit in **17** and **18** (Section 4). The three strong carbonyl stretching absorptions in **14a** and **14b** are characteristic for this type of metal carbonyl building block [9]. For the iron–platinum molecules **10a**, **10b** and **12** two stretching frequencies at ca. 2210 ($\nu_{C\equiv CFc}$) and 2078 cm^{-1} ($\nu_{C\equiv CPt}$) are found, which is consistent with the two different alkynyl carbon–carbon triple bonds present (Section 4) [7,10].

The NMR spectroscopic properties of **4**, **14**, **17** and **18** are consistent with their formulations as heterometallic ruthenium acetylide-based complexes (Section 4). The ^1H NMR spectra of these compounds show resonance signals in the aromatic region typical for pyridine, bipyridine, and phenyl groups. Due to the different chemical environment, the dppf cyclopentadienyl protons appear as four separated signals, whereby three of them are found between 4.0 and 4.4 ppm and the other is located at ca. 5.1 ppm. The coordination of the bipyridine ligand to the respective metal atoms can be verified by the shift of the resonance signals of the bipyridine protons, *i.e.*, due to the coordination of the bipyridine moiety to manganese the protons H6 and H6′, which are located next to the nitrogen atoms, are shifted from 8.42 (H6) and 8.64 ppm (H6′) in **4a** to 8.86

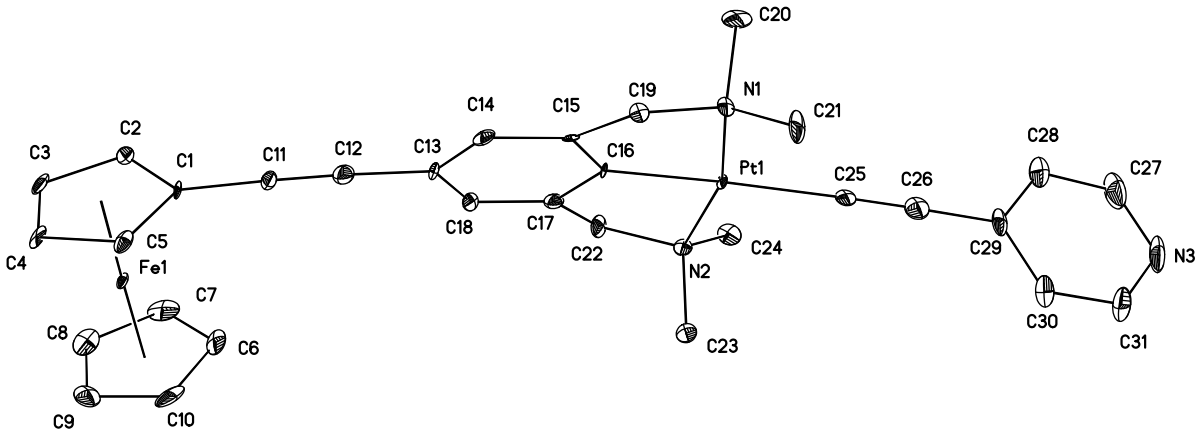

Fig. 1. ORTEP drawing of **10b**. Thermal ellipsoids are shown at 50% probability level. The hydrogen atoms are omitted for clarity. Selected bond lengths (Å) and angles (°): C1–C11, 1.445(6); C11–C12, 1.187(7); C12–C13, 1.448(6); C16–Pt1, 1.949(4); Pt1–N1, 2.091(3); Pt1–N2, 2.093(3); Pt1–C25, 2.062(4); C25–C26, 1.202(7); C26–C29, 1.433(7); Fe1–D1, 1.6433(2); Fe1–D2, 1.6533(2); C1–C11–C12, 178.1(5); C11–C12–C13, 177.1(5); C16–Pt1–C25, 177.84(17); Pt1–C25–C26, 178.9(4); C25–C26–C29, 176.4(5); N1–Pt1–N2, 163.06(14); C16–Pt1–N1, 81.35(16); C16–Pt1–N2, 81.71(16); N1–Pt1–C25, 98.74(15); N2–Pt1–C25, 98.19(15); (D1 = centroid of C_5H_4; D2 = centroid of C_5H_5).

(H6) and 9.16 ppm (H6′) in **14a** [9,11]. Notable in the ^{1}H NMR spectra of **17** and **18**, when compared with **15** and **16**, is the highfield shift of the $Me_3SiC{\equiv}C$ protons from ca. 0.25 ppm (**15**) to −0.45 (**17**) and −0.28 ppm (**18**), respectively, which can be explained by the ring current of the bipyridine ligand [11]. Furthermore, **17a** and **17b** show two separated resonance signals for the Me_3Si protons of the titanium-bonded cyclopentadienyl ligands which is attributed to their unsymmetrical chemical environment (Section 4) [11]. The protons of the Me_2NCH_2 pincer arms in **10** are observed at ca. 3.20 (NMe_2) and 4.12 ppm (CH_2) showing typical ^{195}Pt satellites with coupling constants of ca. 40 Hz ($^{3}J_{PtH(Me)}$ and $^{3}J_{PtH(CH2)}$) [7,10]. The successful formation of **12** is evidenced by a

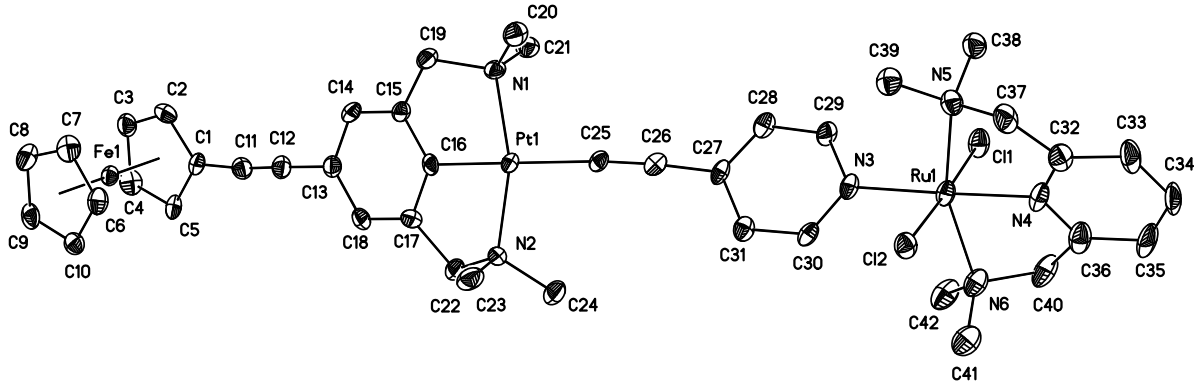

Fig. 2. ORTEP drawing of one of the two crystallographically independent molecules of **12**. Thermal ellipsoids are shown at 30% probability level. The hydrogen atoms and the three dichloromethane solvent molecules are omitted for clarity. Selected bond lengths (Å) and angles (°): C1–C11, 1.420(19); C11–C12, 1.189(19); C12–C13, 1.463(19); C16–Pt1, 1.949(13); Pt1–N1, 2.077(10); Pt1–N2, 2.065(10); Pt1–C25, 2.026(13); C25–C26, 1.238(18); C26–C27, 1.431(17); Fe1–D1, 1.652(6); Fe1–D2, 1.642(6); Ru1–N3, 2.112(10); Ru1–N4, 1.981(11); Ru1–N5, 2.212(11); Ru1–N6, 2.187(12); Ru1–Cl1, 2.413(4); Ru1–Cl2, 2.421(3); C1–C11–C12, 174.5(15); C11–C12–C13, 178.1(15); C16–Pt1–C25, 173.6(5); Pt1–C25–C26, 171.7(11); C25–C26–C27, 174.8(14); N1–Pt1–N2, 162.3(4); C16–Pt1–N1, 81.4(5); C16–Pt1–N2, 81.0(5); N1–Pt1–C25, 98.6(4); N2–Pt1–C25, 99.1(5); N3–Ru1–N4, 178.4(5); N5–Ru1–N6, 158.6(4); Cl1–Ru1–Cl2, 177.81(12); N3–Ru1–N5, 99.4(4); N3–Ru1–N6, 102.0(4); N4–Ru1–N5, 79.1(5); N4–Ru1–N6, 79.5(5); (D1 = centroid of C_5H_4; D2 = centroid of C_5H_5).

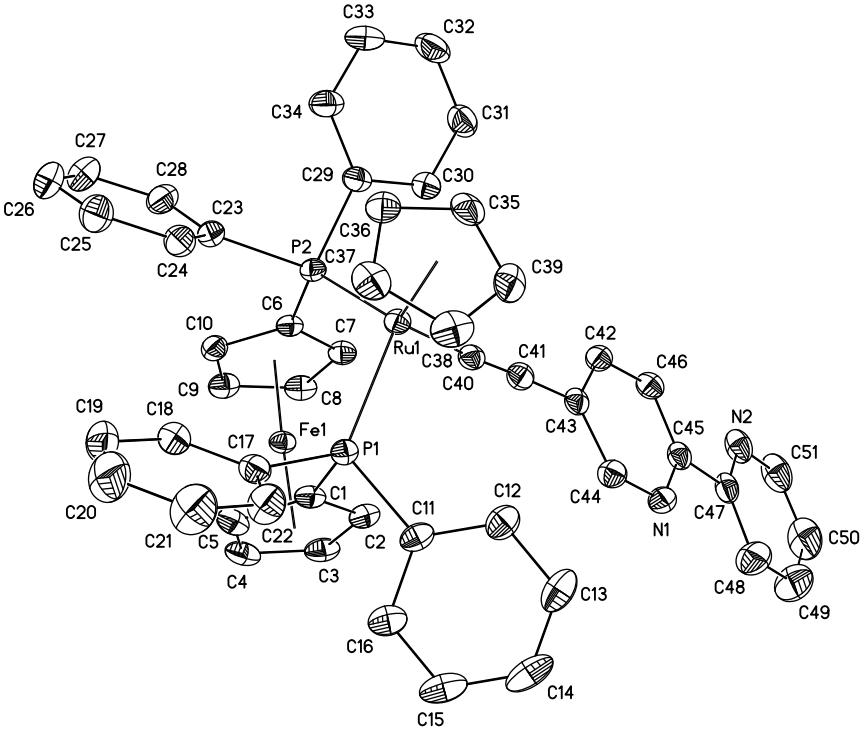

Fig. 3. ORTEP drawing of **4b**. Thermal ellipsoids are shown at 50% probability level. The hydrogen atoms and the non-coordinated dichloromethane solvent molecule are omitted for clarity. Selected bond lengths (Å) and angles (°): Ru1–P1, 2.2677(5); Ru1–P2, 2.2774(5); Ru1–C40, 2.0029(18); C40–C41, 1.208(3); C41–C43, 1.429(2); Ru1–D1, 1.8888(8); Fe1–D2, 1.6413(8); Fe1–D3, 1.6391(8); P1–Ru1–P2, 97.061(17); Ru1–C40–C41, 173.04(15); C40–C41–C43, 176.7(2) (D1 = centroid of C_5H_5; D2 = centroid of C1–C5; D3 = centroid of C6–C10).

downfield shift of the pyridine protons adjacent to nitrogen by 1.0 ppm. The pincer ligand at ruthenium additionally shows the expected resonance signals [12].

The $^{31}P\{^{1}H\}$ NMR spectra of all ruthenium–acetylide complexes display one resonance signal at ca. 49 or 54 ppm, due to the presence of the PPh_3 or dppf units [4,5,13]. Coordination of the bipyridine ligand to the respective transition metal fragments in **14**, **17** and **18** does not significantly influence the position of these signals (Section 4).

The identity of heterobimetallic **10a** and **10b** and heterotrimetallic **12** was additionally evidenced from the mass spectrometric investigations. The electrospray ionization mass spectra (ESI MS) show the molecular ion peaks at a mass-to-charge ratio of 774.4 $[\mathbf{10a}+H]^+$, 697.3 $[\mathbf{10b}+H]^+$ and 1062.4 $[\mathbf{12}+H]^+$. The mass and isotope distribution patterns comply to the formulated structures.

2.2. Structural characterization

Complexes **4b**, **10b**, **12** and **17b** were further characterized by single crystal X-ray diffraction studies. The molecular structures of these molecules are shown in Figs. 1–4. Selected bond distances (Å) and angles (°) are given in the legends of Figs. 1–4, while the crystal and structure refinement data are summarized in Table 1 (Section 4).

Single crystals of **10b** for X-ray structure analysis were obtained by layering a dichloromethane/acetonitrile solution containing **10b** with *n*-pentane. Complex **10b** crystallizes in the monoclinic space group $P2_1/n$. The main structural features resemble the structural data characteristic for ferrocene and NCN pincer complexes [7,15,16]. Consistent with other ferrocene complexes the Fe1–D1 and Fe1–D2 separations are found with 1.6433(2) and 1.6533(2) Å [15]. The two cyclopentadienyl ligands are rotated by 2.35(9)° to each other, which verifies an almost eclipsed conformation.

The Pt1 atom adopts a distorted square-planar geometry set-up by C16, N1, N2 and C25 (r.m.s. deviation 0.0168 Å). The C16–Pt1–C25 bond angle is with 177.84(17)° almost linear, while the N1–Pt1–N2 angle with 163.06(14)° deviates from linearity. The C≡C functionalities are as expected linear (C1–C11–C12, 178.1(5)°; C11–C12–C13, 177.1(5)°; Pt1–C25–C26, 178.9(4)°; C25–C26–C29, 176.4(5)°). Notable is the angle between the planes of the C_6H_2 unit, the pyridine entity and the η^5-coordinated C_5H_4 ring. For the C_6H_2 and the cyclopentadienyl ring a tilting angle of 61.70(1)° is found, while between

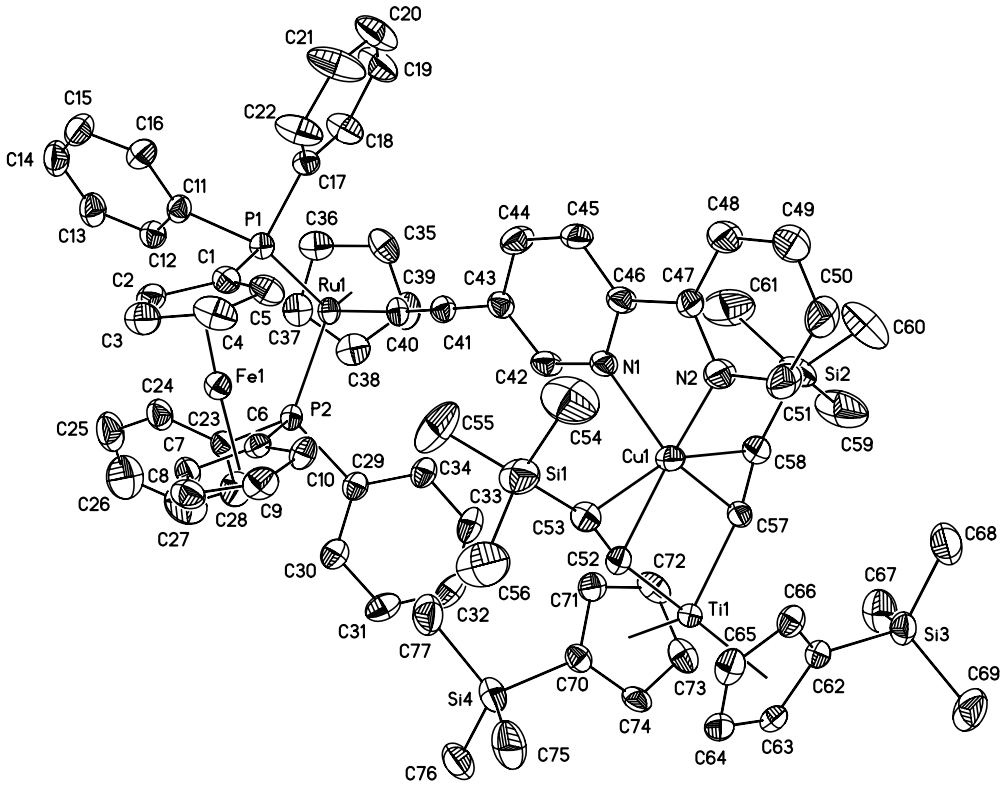

Fig. 4. The molecular structure (ORTEP 30% probability level) of heterotetrametallic **17b** with the atomic numbering scheme. Hydrogen atoms, the solvent molecule tetrahydrofuran and the PF_6^- counter ion are omitted for clarity. Selected bond distances (Å) and angles (°): Ru1–P1, 2.2985(13); Ru1–P2, 2.2758(13); Ru1–C40, 2.004(5); C40–C41, 1.200(6); C41–C43, 1.440(7); Ru1–D1, 1.9006(2); Fe1–D2, 1.6392(2); Fe1–D3, 1.6312(2); Ti1–D4, 2.0570(2); Ti1–D5, 2.0476(2); Ti1–C52, 2.101(5); Ti1–C57, 2.091(5); C52–C53, 1.227(6); C57–C58, 1.237(6); Cu1–N1, 2.115(4); Cu1–N2, 2.123(4); P1–Ru1–P2, 98.46(5); Ru1–C40–C41, 175.9(4); C40–C41–C43, 178.4(5); C52–Ti1–C57, 89.10(18); Ti1–C52–C53, 168.2(4); Ti1–C57–C58, 168.2(4); C52–C53–Si1, 162.6(4); C57–C58–Si2, 160.1(5); N1–Cu1–N2, 77.92(15) (D1 = centroid of C_5H_5; D2 = centroid of C1–C5; D3 = centroid of C6–C10; D4 = centroid of C62–C66; D5 = centroid of C70–C74).

Table 1
Crystal and intensity collection data for **4b**, **10b**, **12** and **17b**

	4b	**10b**	**12**	**17b**
Empirical formula	$C_{52}H_{42}Cl_2FeN_2P_2Ru$	$C_{31}H_{31}FeN_3Pt$	$C_{88}H_{108}Cl_{12}Fe_2N_{12}Pt_2Ru_2$	$C_{81}H_{92}CuF_6FeN_2OP_3RuSi_4Ti$
Formula weight	984.64	696.53	2463.28	1697.20
Crystal system	Monoclinic	Monoclinic	Triclinic	Monoclinic
Space group	$P2_1/c$	$P2_1/n$	$P\bar{1}$	$P2_1$
a (Å)	11.2769(5)	5.80820(10)	12.681(2)	16.5178(14)
b (Å)	28.6778(13)	11.89020(10)	12.7005(13)	14.4734(12)
c (Å)	14.2622(7)	37.6944(3)	30.778(6)	17.4078(15)
α (°)	90	90	96.359(12)	90
β (°)	107.1530(10)	93.0220(10)	91.404(15)	93.195(2)
γ (°)	90	90	92.345(11)	90
V (Å^3)	4407.2(4)	2599.58(5)	4920.4(14)	4155.2(6)
ρ_{calc} (g cm^{-3})	1.484	1.780	1.663	1.357
$F(000)$	2008	1368	2440	1752
Crystal dimensions (mm^3)	0.5 × 0.3 × 0.1	0.5 × 0.2 × 0.2	0.5 × 0.2 × 0.1	0.3 × 0.2 × 0.03
Z	4	4	2	2
Maximum, minimum transmission	0.99999, 0.847974	1.00000, 0.25740	1.00000, 0.18909	0.99999, 0.781845
Absorption coefficient (μ, mm^{-1})	0.905	14.576	13.281	0.867
Scan range (°)	1.42–27.10	3.90–60.51	3.49–60.25	1.65–26.38
Index ranges	$-14 \leqslant h \leqslant 13$, $0 \leqslant k \leqslant 36$, $0 \leqslant l \leqslant 18$	$-6 \leqslant h \leqslant 6$, $-13 \leqslant k \leqslant 13$, $-42 \leqslant l \leqslant 42$	$-14 \leqslant h \leqslant 13$, $-14 \leqslant k \leqslant 14$, $-34 \leqslant l \leqslant 34$	$-20 \leqslant h \leqslant 20$, $-18 \leqslant k \leqslant 18$, $0 \leqslant l \leqslant 21$
Total reflections	53,441	18,805	33,523	47,881
Unique reflections	9946	3918	14,248	17,026
R_{int}	0.0260	0.0291	0.0477	0.0616
Data/restraints/parameters	9725/0/541	3918/24/325	14248/96/1119	17005/46/922
Goodness-of-fit on F^2	1.039	1.203	1.079	1.014
R_1,[a] wR_2^a [$I \geqslant {}^3 2\sigma(I)$]	0.0263, 0.0635	0.0278, 0.0694	0.0708, 0.1744	0.0436, 0.0851
R_1,[a] wR_2^a (all data)	0.0311, 0.0662	0.0284, 0.0697	0.0842, 0.1813	0.0810, 0.0995
Maximum, minimum peak in final Fourier map (e Å^{-3})	0.832, −0.922	1.015, −0.991	3.900, −1.596	0.387, −0.402

n, the number of reflections; p, the parameters used.
[a] [a] $R_1 = [\sum(||F_o| - |F_c|)/\sum(|F_o|)$; $wR_2 = [\sum(w(F_o^2 - F_c^2)^2)/\sum(wF_o^4)]^{1/2}$. $S = [\sum w(F_o^2 - F_c^2)^2]/(n-p)1/2$.

the C_6H_2 moiety and the pyridine unit an angle of 83.34(1)° is typical. These orientations avert an optimal overlap between the π-orbitals, but primarily seem to depend on crystal packing effects.

Complex **12** crystallized by the diffusion of *n*-pentane into a dichloromethane solution containing **12** at −30 °C as deep red needles. Compound **12** crystallizes in the triclinic space group $P\bar{1}$ with two crystallographically independent molecules in the asymmetric unit. The result of the X-ray diffraction study confirms the general structure of **12**, suggested on the basis of the IR and ^{1}H NMR data. With minor deviations the structural properties of the Fc–C≡C–NCN–Pt–C≡C–C_5H_4N unit are comparable to that found for **10b**.

The ruthenium(II) centre occupies a distorted octahedral surrounding, with the three N-donor atoms of the NN′N ligand in a meridional position. The introduced pyridine ligand is σ-coordinated via the nitrogen atom and positioned *trans* to the pyridine nitrogen atom of the *NN′N* ligand, a situation which forces the two chloride ligands *trans* to each other in the apical positions. The Ru–N_{py}, Ru–N_{NMe} and Ru–Cl distances as well as the angles around the Ru(II) ion (Fig. 2) are consistent with those values reported for this type of building block [17]. The Ru1–N3 bond distance (2.112(10) Å) is elongated when compared to that of Ru1–N4 (1.981(11) Å), but both lie in the range of distances reported for other ruthenium(II)–pyridine complexes [17,18]. The angle N3–Ru1–N4 (178.4(5) Å) illustrates the linearity of this array. The planes of the two pyridine rings form a tilting angle of 64.72(0.49)° with respect to each other. The calculated overall length of molecule **12** amounts to ca. 25.88 Å (C9–C34).

Molecule **4b** crystallizes in the monoclinic space group $P2_1/c$. The overall structural features of **4b** are similar to those of the related structurally characterized diphenylphosphino ferrocene, cyclopentadienyl ruthenium σ-acetylides and bipyridine-containing compounds with ruthenium in a pseudo-tetrahedral arrangement [4,5,11,13,14]. The cyclopentadienyl rings of the dppf entity are rotated by 2.13(4)° to each other which verifies an almost eclipsed conformation. The ruthenium acetylide unit Ru1–C40–C41–C43 is with 173.04(15)° (Ru1–C40–C41) and 176.7(2)° (C40–C41–C43) almost linear. Notable is the dppf bite angle P1–Ru1–P2 which is with 97.061(17)° smaller than those ones found in (η^5-C_5H_5)(Ph_3P)$_2$Ru σ-acetylides (99.01(6)–101.17(7)°), but similar to the related (dppf)(η^5-C_5H_5)Ru–acetylide systems [5,13]. The ruthenium–phosphorus distances are with 2.2677(5) (Ru1–P1) and 2.2774(5) Å (Ru1–P2) characteristic of this type of

molecules [5,13]. The same is true for the Ru1–C40, C40–C41 and C41–C43 separations (Fig. 3).

Single crystals of **17b** suitable for X-ray diffraction studies could be grown by the slow vapour diffusion of *n*-pentane into a tetrahydrofuran solution containing **17b** at −30 °C. Fig. 4 shows the perspective drawing of **17b** together with the atomic numbering scheme. Heterotetrametallic **17b** crystallizes in the monoclinic space group $P2_1$. The molecular structure of **17b** consists of a (dppf)(η^5-C_5H_5)Ru–C≡C–bipy building block, the 1,1′-bis(diphenylphosphino)ferrocene unit of which is in a eclipsed geometry (5.93(2)°), and the cyclopentadienyl rings are inclined at an angle of 4.63(0.21)°. The bipyridine moiety in **17b** is chelate-bonded to the organometallic Ti–Cu tweezer fragment [{[Ti](μ–σ,π-C≡CSiMe$_3$)$_2$}Cu]$^+$ (Fig. 4).

The copper(I) ion possesses, as typical for this type of compounds, a pseudo-tetrahedral arrangement [11,19]. The carbon–carbon distances of the ruthenium and titanium acetylide moieties are 1.200(6) (C40–C41), 1.227(6) (C52–C53), and 1.237(6) Å (C57–C58), which are comparable to those of other ruthenium(II) and titanium(IV) alkynyls [4,5,13,19]. The respective Ru–C≡C unit is essentially linear, while the Ti–C≡C–Si moieties are *trans*-bent as expected for heterobimetallic [{[Ti](μ–σ,π-C≡CSiMe$_3$)$_2$}Cu]$^+$ organometallic π-tweezer fragments in which a copper(I) ion is η^2-coordinated by the chelating ligand [Ti](C≡CSiMe$_3$)$_2$ (Fig. 4) [11,19]. The {[Ti](μ–σ,π-C≡CSiMe$_3$)$_2$}Cu]$^+$ unit (Ti1, C52, C53, C57, C58, Cu1; r.m.s. deviation 0.0371 Å) is with 78.78(9)° almost perpendicular oriented to the plane spanned by the bipy entity (N1, N2, C45–C48, Cu1; r.m.s. deviation 0.0919 Å) (Fig. 4). All other bond lengths and angles require no further discussion, because they agree well with those parameters described for related transition metal complexes [4,5,11,13,19].

2.3. Cyclic voltammetry

Complexes **4**, **10b**, **12**, **17** and **18** were investigated by cyclic voltammetry to fathom the interaction of the metal centers concerning their particular redox behavior. The cyclic voltammograms of **10b** and **12** (Fig. 5) show next to the reversible redox process for iron(II) (**10b**: $E_0 = 0.05$ V, $\Delta E_p = 0.11$ V; **12**: $E_0 = 0.06$ V, $\Delta E_p = 0.12$ V) a weak irreversible oxidation at ca. 0.65 V the origin of which most likely arises from the oxidation of the NCN pincer unit since this behavior has also been reported for **6** and the parent compound **9** [7,10a,20]. For heterotrimetallic **12** a further reversible oxidation wave is found at $E_0 = -0.42$ V ($\Delta E_p = 0.12$ V) which can be assigned to the Ru(II)/Ru(III) oxidation. This potential is similar to that found in {Ti}(C≡C–C_5H_4N–[Ru]) ({Ti} = (η^5-C_5H_5)$_2$Ti(CH_2SiMe_3)). In comparison with [Ru]–NC_5H_5, the ruthenium oxidation potential of **12** is shifted to a more negative value indicating that the oxidation is facilitated by the presence of a platinum building block in *para*-position [21]. Measuring the cyclic voltammograms upto 1.6 V results in the appearance of an additional irreversible oxidation wave at $E_{p,ox} = 1.27$ V (Fig. 5, bottom) which most probably can be assigned to an oxidation of the 2,6-bis[(dimethylamino)methyl]pyridine ligand at ruthenium.

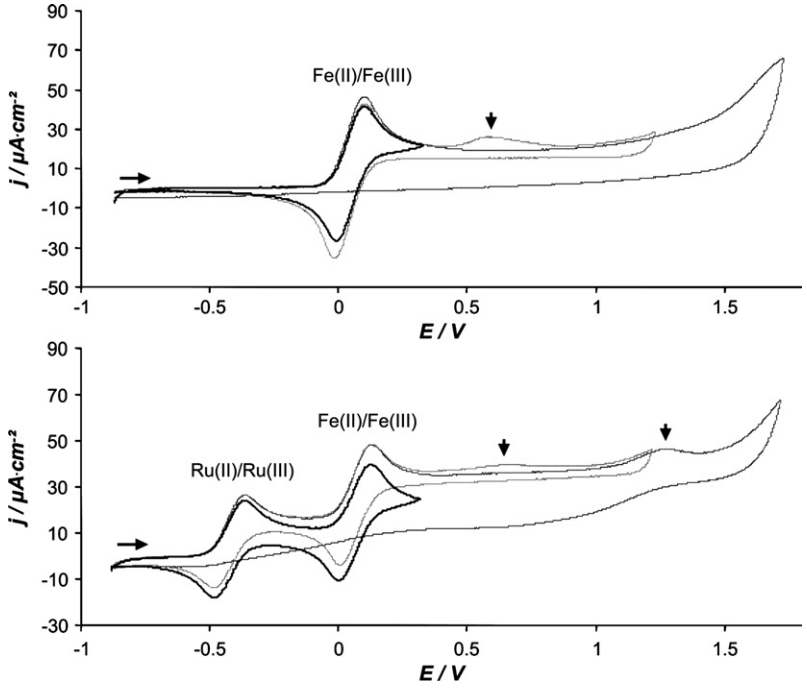

Fig. 5. Representation of the cyclic voltammograms of **10b** (top) and **12** (bottom) in three different potential ranges (10^{-3} M solutions in dichloromethane at 25 °C, [*n*-Bu_4N]PF_6 supporting electrolyte (0.1 M), scan rate = 0.1 V s^{-1}; all potentials are referenced to the FcH/FcH^+ redox couple with $E_0 = 0.00$ V [23,24]).

Table 2
Electrochemical data for **1b**, **4a**, **4b**, **17a**, **17b**, **18a** and **18b**[a]

Compound	Reduction		Oxidation			
	E_0 (ΔE_p) M(I)/M(0)	$E_{p,red}$ M(I)/M(0)	E_0 (ΔE_p) Ru(II)/Ru(III)	E_0 (ΔE_p) Fe(II)/Fe(III)	$E^d_{p,ox}$	$E^d_{p,ox}$
1b			0.09 (0.13)	0.42 (0.14)		
4a			0.07 (0.10)			0.855
4b			0.04 (0.10)	0.51 (0.12)	0.45	0.805
17a	−1.50 (0.11)[b]		0.215 (0.10)			
17b	−1.52 (0.095)[b]		0.20 (0.115)	0.545 (0.165)		
18a		−1.41[c]	0.205 (0.10)			0.91
18b		−1.41[c]	0.205 (0.12)	0.56 (0.16)	0.48	0.86

[a] All potentials are given in V vs. FcH/FcH^+ [23,24] from single scan cyclic voltammograms (10^{-3} M solutions in dichloromethane at 25 °C, [*n*-Bu_4N]PF_6 supporting electrolyte (0.1 M), scan rate = 0.1 V s^{-1}). Detailed experimental conditions are listed in Section 4.
[b] M = Cu.
[c] M = Ag.
[d] Irreversible or quasi-reversible redox processes that may result from the oxidation of ruthenium [13a,22].

For both complexes these measurements apparently cause a decomposition of the molecules because no subsequent reduction waves for iron(III) and ruthenium(III) could be observed (Fig. 5).

The electrochemical data for **4**, **17** and **18** are presented in Table 2. The Ru(II)/Ru(III) oxidation in the ruthenium σ-acetylides **4a** and **4b** is found at $E_0 = 0.07$ V (**4a**) and $E_0 = 0.04$ V (**4b**) with $\Delta E_p = 0.10$ V. While free dppf reveals a reversible oxidation wave at $E_0 = 0.190$ V [5], its Fe(II)/Fe(III) oxidation is positive shifted to 0.42 V in [(η^5-C_5H_5)(dppf)RuCl] (**1b**) in which the oxidation of Ru(II) to Ru(III) takes place at 0.09 V. Compared to that the redox potentials of the Ru(II) and Fe(II) ions in **4b** show small negative and positive shifts, respectively. Although the additionally observed oxidation processes in complexes **4a** and **4b** are not reversible, they may originate from the oxidation of the ruthenium center, which can be verified by a comparison to other complexes containing (η^5-C_5H_5)(PPh_3)$_2$Ru or (η^5-C_5H_5)(dppf)Ru termini [13a,22]. The Fe(II)/Fe(III) redox process in **4b** could be assigned since its potential is close to that of the iron(II) ion in [(η^5-C_5H_5)(dppf)RuCl] (**1b**) [5,13a].

The coordination of the bipyridine ligand to a bis(alkynyl)titanocene–copper(I) or -silver(I) fragment as given in complexes **17** and **18** causes a positive shift for the Ru(II)/Ru(III) redox couple of about 0.15 V (Fig. 6).

Along with the above mentioned more difficult oxidation of ruthenium in **17** and **18** as a result of the introduction of the π-tweezer building block, consequently the reduction of the Cu(I) and Ag(I) centers is somewhat different and hence, more complicated. This is illustrated by a shift of the reduction current peak to a more negative value (Table 2), when compared with, for example, [FcC≡C–bipy{[Ti](μ–σ,π-C≡CSiMe_3)$_2$}M]X (M = Cu, X = PF_6: $E_0 = -1.39$ V ($\Delta E_p = 0.12$ mV); M = Ag, X = ClO_4: $E_{p,red} = -1.26$ V) [11].

This observation also corresponds to the IR data of these systems, where, compared to **4**, a decreased electron density at the RuC≡C moiety is present in **17** and **18**, which is evidenced by a shift of the $\nu_{C\equiv C}$ vibration to lower wavenumbers. The Fe(II)/Fe(III) oxidation in **17b** and **18b** is thereby only slightly affected by copper(I) or silver(I) (Table 2). The additionally observed oxidation processes for complexes **18a** and **18b** are comparable to those found in **4a** and **4b** and consequently can be referred to oxidations at the ruthenium center [13a,22]. Due to the electrochemical window of dichloromethane the expected reduction of the pendant bipyridine unit could not be observed.

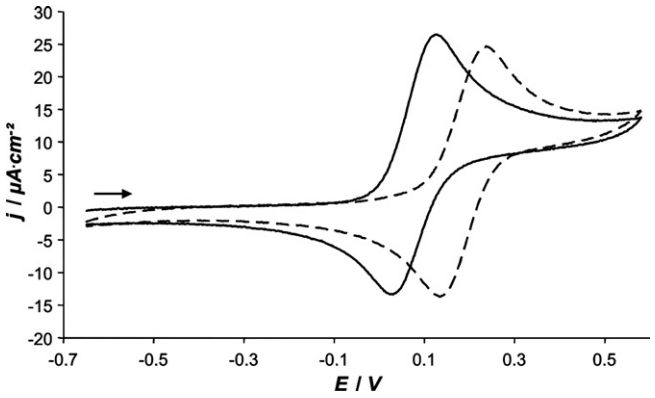

Fig. 6. Comparison of the Ru(II)/Ru(III) redox couples of **4a** (–) and **18a** (---), respectively, in the oxidative region of the cyclic voltammogram (10^{-3} M solutions in dichloromethane at 25 °C, [*n*-Bu_4N]PF_6 supporting electrolyte (0.1 M), scan rate = 0.1 V s^{-1}; all potentials are referenced to the FcH/FcH^+ redox couple with $E_0 = 0.00$ V [23,24]).

3. Conclusions

A series of heterometallic complexes with two, three, and four different transition metal atoms, such as titanium, manganese, iron, ruthenium, platinum, and copper is described. Following organometallic species (η^5-C_5H_5)L_2Ru–C≡C–bipy (L = PPh_3, L_2 = dppf; bipy = 2,2′-bipyridine-5-yl; dppf = 1,1′-bis(diphenylphosphino)ferrocene), Fc–C≡C–NCN–Pt–C≡C–R (R = bipy, C_5H_4N-4; Fc = (η^5-C_5H_5)(η^5-C_5H_4)Fe; NCN = [C_6H_2(CH_2NMe_2)$_2$-2,6]$^-$), Fc–C≡C–NCN–Pt–C≡C–C_5H_4N–[Ru] ([Ru] = [η^3-*mer*-{2,6-(Me_2NCH_2)$_2$$C_5H_3N$}$RuCl_2$]), ($\eta^5$-$C_5H_5$)$L_2$Ru–C≡C–bipy[$Mn(CO)_3Br$] and ($\eta^5$-$C_5H_5$)$L_2$Ru–C≡C–bipy[{[Ti](μ–σ,π-C≡CSiMe_3)$_2$}M]X (M = Cu, Ag; X =

PF_6, BF_4, ClO_4) were prepared by combining different organic and organometallic building blocks of lower nuclearity from a ligand and coordination complex library particularly designed and built up for this purpose. In these species the appropriate transition metals are connected by carbon-rich bridging units based on alkynyls, cyclopentadienyl and bipyridine moieties. These complexes add to the so far only less investigated family of heteromultimetallic transition metal complexes.

Investigation of the redox chemistry of the selected complexes revealed an electronic influence of the appropriate metal building blocks on each other, which could be demonstrated by cyclic voltammetry.

4. Experimental

4.1. General methods

All reactions were carried out under an atmosphere of purified nitrogen using standard Schlenk techniques. Tetrahydrofuran, diethyl ether, petroleum ether and *n*-hexane were purified by distillation from sodium/benzophenone ketyl. Diisopropylamine was dried by distillation from KOH. Methanol was dried with magnesium and dichloromethane was distilled from CaH_2. Infrared spectra were recorded with a Perkin–Elmer FT-IR 1000 spectrometer. NMR spectra were recorded with a Bruker Avance 250 spectrometer (^{1}H NMR at 250.12 MHz and $^{13}C\{^1H\}$ NMR at 62.86 MHz) in the Fourier transform mode. Chemical shifts are reported in δ units (parts per million) downfield from tetramethylsilane ($\delta = 0.00$ ppm) with the solvent as the reference signal ($CDCl_3$: ^{1}H NMR, $\delta = 7.26$; $^{13}C\{^1H\}$ NMR, $\delta = 77.16$) [25]. $^{31}P\{^1H\}$ NMR spectra were recorded at 101.255 MHz in $CDCl_3$ with $P(OMe)_3$ as the external standard ($\delta = 139.0$, rel. to H_3PO_4 (85%) with $\delta = 0.00$ ppm). ESI-TOF mass spectra were recorded using a Mariner biospectrometry workstation 4.0 (Applied Biosystems). Cyclic voltammograms were recorded in a dried cell purged with purified argon at 25 °C. Platinum wires served as the working electrode and the counter electrode. A saturated calomel electrode served as the reference electrode. For the ease of comparison, all potentials are converted using the redox potential of the ferrocene–ferrocenium couple Cp_2Fe/Cp_2Fe^+ ($Cp_2Fe = (\eta^5\text{-}C_5H_5)_2Fe$) as the reference ($E_0 = 0.00$ V) [23]. A conversion of the given data to the standard normal hydrogen electrode is possible following the suggestion made by Strehlow et al. [24]. Electrolyte solutions were prepared from freshly distilled dichloromethane solutions and $[n\text{-}Bu_4N]PF_6$ ($c = 0.1$ M). The appropriate organometallic complexes were added at $c = 1$ mM. Cyclic voltammograms were recorded at a scan rate of 100 mV s^{-1} using a Radiometer Copenhagen DEA 101 Digital Electrochemical analyzer with an IMT 102 Electrochemical Interface. Melting points were determined using sealed nitrogen purged capillaries on a Gallenkamp MFB 595 010 M melting point apparatus. Microanalyses were performed with a CHN-analyzer FLASHEA 1112 Series (Thermo) by the Department of Inorganic Chemistry at Chemnitz, Technical University.

4.2. General remarks

$(\eta^5\text{-}C_5H_5)(PPh_3)_2RuCl$ [26], $(\eta^5\text{-}C_5H_5)$(dppf)RuCl [27], 5-ethynyl-2,2′-bipyridine [28], 4-ethynylpyridine [29], [Ru]N≡N[Ru] [8], $Mn(CO)_5Br$ [30], [{[Ti](μ–σ,π-C≡CSiMe_3)$_2$}Cu(N≡CMe)]PF_6 [31], [{[Ti](μ–σ,π-C≡CSiMe_3)$_2$}-Cu(N≡CMe)]BF_4 [31], {[Ti](μ–σ,π-C≡CSiMe_3)$_2$}$AgOClO_3$ [32], Fc–C≡C–NCNH [7] and Fc–C≡C–NCNPtCl [7] were prepared following published procedures. All other chemicals were purchased from commercial suppliers and were used as received.

4.3. Synthesis of $(\eta^5\text{-}C_5H_5)(PPh_3)_2Ru\text{–}C{\equiv}C\text{–}bipy$ (**4a**)

About 160 mg (0.89 mmol) of 5-ethynyl-2,2′-bipyridine (**2**) dissolved in MeOH (20 mL) was added to 600 mg (0.83 mmol) of $(\eta^5\text{-}C_5H_5)(PPh_3)_2RuCl$ (**1a**) and 140 mg (0.86 mmol) of NH_4PF_6 in dichloromethane (20 mL). The reaction mixture was stirred at 25 °C for 20 h, whereby the color of the solution changed from orange to deep red. Afterwards all volatile materials were removed in oil-pump vacuum and the remaining residue was dissolved in dichloromethane and filtered through a pad of Celite. Removal of the solvent under reduced pressure gave **3a** as a dark red solid which was re-dissolved in tetrahydrofuran (30 mL). Afterwards 1,8-diazabicyclo[5.4.0]undec-7-ene (DBU, 0.15 mL, 1.0 mmol) was added dropwise, resulting in a color change from red to yellow. Stirring was continued for 1 h at 25 °C and all volatiles were removed under reduced pressure. The residue was chromatographed under nitrogen on silica gel. Eluting with tetrahydrofuran/*n*-hexane (1:3, v/v) provided a yellow band from which **4a** could be isolated as a yellow solid. Yield: 490 mg (0.56 mmol, 68% based on **1a**).

3a: IR (KBr, cm^{-1}): 2038m ($\nu_{C\equiv C}$), 1624m ($\nu_{C=C}$), 842s (ν_{P-F}). $^{31}P\{^1H\}$ NMR ($CDCl_3$): [δ] 49.1 (s, PPh_3), 39.2 (s, PPh_3), −145.1 (septet, $^1J_{PF} = 713$ Hz).

4a: M.p.: >185 °C (decomp.). IR (KBr, cm^{-1}): 2070s ($\nu_{C\equiv C}$). ^{1}H NMR ($CDCl_3$): [δ] 4.36 (s, 5H, C_5H_5), 7.05–7.25 (m, 19H, C_6H_5 + *H5′*/bipy), 7.37–7.50 (m, 13H, C_6H_5 + *H4*/bipy), 7.77 (ddd, $^3J_{H4'H3'} = {}^3J_{H4'H5'} = 7.8$ Hz, $^4J_{H4'H6'} = 1.8$ Hz, 1H, *H4′*/bipy), 8.15 (dd, $^3J_{H3H4} = 8.4$ Hz, $^5J_{H3H6} = 0.8$ Hz, 1H, *H3*/bipy), 8.32 (ddd, $^3J_{H3'H4'} = 7.8$ Hz, $^4J_{H3'H5'} = 1$ Hz, $^5J_{H3'H6'} = 1$ Hz, 1H, *H3′*/bipy), 8.42 (dd, $^4J_{H6H4} = 2.2$ Hz, $^5J_{H6H3} = 0.8$ Hz, 1H, *H6*/bipy), 8.64 (ddd, $^3J_{H6'H5'} = 4.8$ Hz, $^4J_{H6'H4'} = 1.8$ Hz, $^5J_{H6'H3'} = 1$ Hz, 1H, *H6′*/bipy). $^{13}C\{^1H\}$ NMR ($CDCl_3$): [δ] 85.5 (t, $J_{CP} = 2$ Hz, C_5H_5), 112.2 (C^i/bipy), 120.2 (*CH*/bipy), 120.7 (*CH*/bipy), 122.7 (*CH*/bipy), 127.4 (pt, $J_{CP} = 4.5$ Hz, CH/C_6H_5), 128.7 (CH/C_6H_5), 133.9 (pt, $J_{CP} = 5$ Hz, CH/C_6H_5), 136.8 (*CH*/bipy), 137.9 (*CH*/bipy), 138.7 (dd, $J_{CP} = 21.5$ Hz, $J_{CP} = 20.5$ Hz, C^i/C_6H_5), 149.1 (*CH*/bipy), 149.7 (C^i/bipy), 151.2 (*CH*/bipy), 156.9 (C^i/bipy). $^{31}P\{^1H\}$ NMR ($CDCl_3$): [δ] 49.2 (s, PPh_3).

Anal. Calc. for $C_{53}H_{42}N_2P_2Ru$ (869.95): C, 73.17; H, 4.87; N, 3.22. Found: C, 72.77; H, 4.75; N, 3.09%.

4.4. Synthesis of (η^5-C_5H_5)(dppf)Ru–C≡C–bipy (**4b**)

Complex **4b** was synthesized by the same procedure as described for the synthesis of **4a**, except that **1b** was used instead of **1a**. Experimental details: (η^5-C_5H_5)(dppf)RuCl (**1b**) (250 mg, 0.33 mmol), 5-ethynyl-2,2′-bipyridine (**2**) (70 mg, 0.39 mmol), NH_4PF_6 (60 mg, 0.37 mmol), 1,8-diazabicyclo[5.4.0]undec-7-ene (DBU, 0.1 mL, 0.67 mmol). Yield: 255 mg (0.28 mmol, 86% based on **1b**).

3b: IR (KBr, cm^{-1}): 2037m ($\nu_{C\equiv C}$), 1635m ($\nu_{C=C}$), 842s (ν_{P-F}). $^{31}P\{^1H\}$ NMR ($CDCl_3$): [δ] 54.0 (s, dppf), 51.9 (s, dppf), −145.1 (septet, $^1J_{PF} = 713$ Hz).

4b: M.p.: 193 °C. IR (KBr, cm^{-1}): 2068s ($\nu_{C\equiv C}$). ^1H NMR ($CDCl_3$): [δ] 3.99 (br s, 2H, C_5H_4), 4.17 (br s, 2H, C_5H_4), 4.32 (br s, 2H, C_5H_4), 4.35 (s, 5H, C_5H_5), 5,24 (br s, 2H, C_5H_4), 7.22 (ddd, $^3J_{H5'H4'} = 7.5$ Hz, $^3J_{H5'H6'} = 4.8$ Hz, $^4J_{H5'H3'} = 1$ Hz, 1H, *H5′*/bipy), 7.28–7.45 (m, 13H, C_6H_5 + *H4*/bipy), 7.50–7.59 (m, 4H, C_6H_5), 7.77 (ddd, $^3J_{H4'H3'} = {}^3J_{H4'H5'} = 7.5$Hz, $^4J_{H4'H6'} = 1.8$ Hz, 1H, *H4′*/bipy), 7.81–7.90 (m, 4H, C_6H_5), 8.22 (dd, $^3J_{H3H4} = 8.4$ Hz, $^5J_{H3H6} = 0.8$ Hz, 1H, *H3*/bipy), 8.33 (ddd, $^3J_{H3'H4'} = 7.5$ Hz, $^4J_{H3'H5'} = 1$ Hz, $^5J_{H3'H6'} = 1$ Hz, 1H, *H3′*/bipy), 8.53 (dd, $^4J_{H6H4} = 2.2$ Hz, $^5J_{H6H3} = 0.8$ Hz, 1H, *H6*/bipy), 8.65 (ddd, $^3J_{H6'H5'} = 4.8$ Hz, $^4J_{H6'H4'} = 1.8$ Hz, $^5J_{H6'H3'} = 1$ Hz, 1H, *H6′*/bipy). $^{13}C\{^1H\}$ NMR ($CDCl_3$): [δ] 68.1 (pt, $J_{CP} = 2.4$ Hz, *CH*/C_5H_4), 71.4 (pt, $J_{CP} = 3$ Hz, *CH*/C_5H_4), 73.2 (pt, $J_{CP} = 2$ Hz, *CH*/C_5H_4), 76.4 (pt, $J_{CP} = 5$ Hz, *CH*/C_5H_4), 84.9 (t, $J_{CP} = 2.4$ Hz, C_5H_5), 88.6 (dd, $J_{CP} = 24.5$ Hz, $J_{CP} = 23.5$ Hz, C^i/C_5H_4), 110.5 (C^i/bipy), 120.8 (*CH*/bipy), 121.0 (*CH*/bipy), 127.3 (pt, $J_{CP} = 4.8$ Hz, *CH*/C_6H_5), 127.4 (pt, $J_{CP} = 4.8$ Hz, *CH*/C_6H_5), 128.9 (*CH*/C_6H_5), 129.3 (*CH*/C_6H_5), 133.9 (pt, $J_{CP} = 5.8$ Hz, *CH*/C_6H_5), 134.2 (pt, $J_{CP} = 5.8$ Hz, *CH*/C_6H_5), 136.8 (*CH*/bipy), 138.1 (*CH*/bipy), 140.8 (dd, $J_{CP} = 21.5$ Hz, $J_{CP} = 20.5$ Hz, C^i/C_6H_5), 141.8 (dd, $J_{CP} = 23.5$ Hz, $J_{CP} = 22.5$ Hz, C^i/C_6H_5), 149.5 (*CH*/bipy), 150.1 (C^i/bipy), 151.6 (*CH*/bipy), 157.1 (C^i/bipy). $^{31}P\{^1H\}$ NMR ($CDCl_3$): [δ] 54.0 (s, PPh_2). Anal. Calc. for $C_{51}H_{40}N_2P_2FeRu$ (899.76): C, 68.08; H, 4.48; N, 3.11. Found: C, 67.35; H, 4.69; N, 3.01%.

4.5. Synthesis of Fc–C≡C–NCNPt–C≡C–bipy (**10a**)

To a cooled (−78 °C) diethyl ether solution containing 65 mg (0.36 mmol) of 5-ethynyl-2,2′-bipyridine (**2a**) was added 0.22 mL (0.35 mmol) of *n*-BuLi (1.6 M in *n*-hexane). The resulting violet solution was stirred for 30 min at this temperature and then Fc–C≡C–NCNPtCl (**9**) (150 mg, 0.24 mmol) was added in a single portion. The reaction mixture was allowed to warm to 25 °C and stirring was continued for 16 h. All volatile materials were then evaporated in oil-pump vacuum and the residue was re-dissolved in dichloromethane and filtered through a pad of Celite. The solution was concentrated to 3 mL and the addition of *n*-hexane (50 mL) led to the precipitation of the title compound. After washing the precipitate twice with diethyl ether (20 mL), complex **10a** was obtained as a brown solid. (Please notice that **10a** always contained small amounts of unreacted **9**.)

IR (KBr, cm^{-1}): 2208w ($\nu_{C\equiv CFc}$), 2078s ($\nu_{C\equiv CPt}$). ^1H NMR ($CDCl_3$): [δ] 3.24 (s, $^3J_{HPt} = 40$ Hz, 12H, N*Me*$_2$), 4.13 (s, $^3J_{HPt} = 41$ Hz, 4H, C*H*$_2$N), 4.21 (pt, $J_{HH} = 1.9$ Hz, 2H, C_5H_4), 4.22 (s, 5H, C_5H_5), 4.46 (pt, $J_{HH} = 1.9$ Hz, 2H, C_5H_4), 7.06 (s, 2H, C_6H_2), 7.24 (ddd, $^3J_{H5'H4'} = 7.8$ Hz, $^3J_{H5'H6'} = 4.7$ Hz, $^4J_{H5'H3'} = 1$ Hz, 1H, *H5′*/bipy), 7.74–7.81 (m, 2H, *H4,H4′*/bipy), 8.23 (dd, $^3J_{H3H4} = 8.4$ Hz, $^5J_{H3H6} = 0.6$ Hz, 1H, *H3*/bipy), 8.34 (ddd, $^3J_{H3'H4'} = 7.8$ Hz, $^4J_{H3'H5'} = 1$ Hz, $^5J_{H3'H6'} = 1$ Hz, 1H, *H3′*/bipy), 8.65 (ddd, $^3J_{H6'H5'} = 4.7$ Hz, $^4J_{H6'H4'} = 1.8$ Hz, $^5J_{H6'H3'} = 1$ Hz, 1H, *H6′*/bipy), 8.69 (dd, $^4J_{H6H4} = 2.4$ Hz, $^5J_{H6H3} = 0.6$ Hz, 1H, *H6*/bipy). $^{13}C\{^1H\}$ NMR ($CDCl_3$): [δ] 56.1 (N*CH*$_3$), 66.2 (C^i/C_5H_4), 68.7 (*CH*/C_5H_4), 70.0 (C_5H_5), 71.3 (*CH*/C_5H_4), 79.7 (N*CH*$_2$), 86.4 (FcC≡C), 87.5 (FcC≡C), 105.2 (PtC≡*C*), 118.7 (C^i/C_6H_2), 120.2 (*C3*/bipy), 121.0 (*C3′*/bipy), 122.0 (*CH*/C_6H_2), 123.2 (*C5′*/bipy), 125.7 (*C5*/bipy), 136.9 (*C4′*/bipy), 139.1 (*C4*/bipy), 143.4 (Pt*C*≡C), 146.2 (C^i/C_6H_2), 149.2 (*C6′*/bipy), 151.6 (*C2*/bipy), 152.2 (*C6*/bipy), 156.5 (*C2′*/bipy) 167.5 (C^i/C_6H_2). MS (ESI-TOF, *m*/*z*): 774.4 $[M+H]^+$. Anal. Calc. for $C_{36}H_{34}N_4FePt$ (773.62): C, 55.89; H, 4.43; N, 7.24. Found: C, 54.37; H, 4.32; N, 7.47%. (Deviations in the elemental analysis are attributed to small amounts of **9** (vide supra)).

4.6. Synthesis of Fc–C≡C–NCNPt–C≡C–py (**10b**)

Experimental conditions and work-up were identical to those used in the synthesis of **10a**. Experimental details: Fc–C≡C–NCNPtCl (**9**) (150 mg, 0.24 mmol), 4-ethynyl pyridine (40 mg, 0.39 mmol), ^{n}BuLi (0.22 mL, 0.35 mmol, 1.6 M in *n*-hexane). Yield: 75 mg (0.11 mmol, 45%).

M.p.: >195 °C (decomp.). IR (KBr, cm^{-1}): 2212w ($\nu_{C\equiv CFc}$), 2077s ($\nu_{C\equiv CPt}$). ^1H NMR ($CDCl_3$): [δ] 3.20 (s, $^3J_{HPt} = 42$ Hz, 12H, N*Me*$_2$), 4.12 (s, $^3J_{HPt} = 43$ Hz, 4H, C*H*$_2$N), 4.21 (pt, $J_{HH} = 1.9$ Hz, 2H, C_5H_4), 4.22 (s, 5H, C_5H_5), 4.45 (pt, $J_{HH} = 1.9$ Hz, 2H, C_5H_4), 7.05 (s, 2H, C_6H_2), 7.19–7.23 (m, 2H, C_5H_4N), 8.37–8.40 (m, 2H, C_5H_4N). $^{13}C\{^1H\}$ NMR ($CDCl_3$): [δ] 56.1 (N*CH*$_3$), 66.2 (C^i/C_5H_4), 68.7 (*CH*/C_5H_4), 70.0 (C_5H_5), 71.3 (*CH*/C_5H_4), 79.7 (N*CH*$_2$), 86.4 (FcC≡C), 87.4 (FcC≡C), 106.4 (PtC≡*C*), 118.9 (C^i/C_6H_2), 122.1 (*CH*/C_6H_2), 126.2 (*CH*/C_5H_4N), 136.5 (C^i/C_5H_4N), 145.4 (Pt*C*≡C), 146.2 (C^i/C_6H_2), 149.3 (*CH*/C_5H_4N), 167.3 (C^i/C_6H_2). MS (ESI-TOF, *m*/*z*): 697.3 $[M+H]^+$. Anal. Calc. for $C_{31}H_{31}N_3FePt{\cdot}1/5CH_2Cl_2$ (713.52): C, 52.52; H, 4.44; N, 5.89. Found: C, 52.76; H, 4.46; N, 5.76%.

4.7. Synthesis of Fc–C≡C–NCNPt–C≡C–py–[Ru] (**12**)

To 30 mg (0.04 mmol) of [Ru]N≡N[Ru] (**11**) in 15 mL of dichloromethane were added 55 mg (0.08 mmol) of

Fc–C≡C–NCNPt–C≡C–py (**10b**) in a single portion. The reaction solution was stirred for 3 h at 25 °C, whereby the color of the solution changed from orange to deep red. The solvent was concentrated to 3 mL and the product was precipitated by the addition of 20 mL of *n*-hexane, washed twice with 10 mL portions of diethyl ether and dried in oil-pump vacuum. Complex **7** was obtained as a red solid. Yield: 70 mg (0.07 mmol, 82% based on **11**).

M.p.: >145 °C (decomp.). IR (KBr, cm^{-1}): 2211w ($\nu_{C\equiv CFc}$), 2077s ($\nu_{C\equiv CPt}$). ^1H NMR ($CDCl_3$): [δ] 2.36 (s, 12H, N*Me*$_2$), 3.23 (s, $^3J_{HPt} = 41$ Hz, 12H, N*Me*$_2$), 4.02 (s, 4H, C*H*$_2$N), 4.13 (s, $^3J_{HPt} = 42$ Hz, 4H, C*H*$_2$N), 4.21 (pt, $J_{HH} = 1.9$ Hz, 2H, C_5H_4), 4.22 (s, 5H, C_5H_5), 4.46 (pt, $J_{HH} = 1.9$ Hz, 2H, C_5H_4), 7.06 (s, 2H, C_6H_2), 7.14 (d, $^3J_{HH} = 7.9$ Hz, 2H, C_5H_3N), 7.26–7.31 (m, 2H, C_5H_4N), 7.36 (t, $^3J_{HH} = 7.9$ Hz, 1H, C_5H_3N), 9.38–9.43 (m, 2H, C_5H_4N). MS (ESI-TOF, *m*/*z*): 1062.4 $[M+H]^+$. Anal. Calc. for $C_{42}H_{50}N_6Cl_2FePtRu$ (1061.8): C, 47.51; H, 4.75; N, 7.92. Found: C, 47.41; H, 4.81; N, 7.39%.

4.8. Synthesis of [(η^5-C_5H_5)(PPh_3)$_2$Ru–C≡C–bipy[Mn(CO)$_3$Br] (**14a**)

$Mn(CO)_5Br$ (**13**) (25 mg, 0.091 mmol) and **4a** (75 mg, 0.086 mmol) were dissolved in 20 mL of ethanol and the reaction solution was heated to reflux for 30 min, whereby the color changed from orange to dark red. After cooling the reaction solution to 25 °C the solvent was reduced in volume to 5 mL, and 15 mL of diethyl ether were added. On cooling the resulting solution to −30 °C complex **14a** precipitated. The obtained solid material was washed twice with 10 mL portions of diethyl ether and dried in oil-pump vacuum. Complex **14a** was obtained as a red-brown solid. Yield: 60 mg (0.055 mmol, 64% based on **4a**).

M.p.: >207 °C (decomp.). IR (KBr, cm^{-1}): 2039s ($\nu_{C\equiv C}$), 2018s 1927s 1912s (ν_{CO}). ^1H NMR ($CDCl_3$): [δ] 4.41 (s, 5H, C_5H_5), 7.08–7.46 (m, 31H, C_6H_5 + *H5′*/bipy), 7.60–8.06 (m, 4H, *H3,H3′*,*H4,H4′*/bipy), 8.86 (br s, 1H, *H6*/bipy), 9.16 (br s, 1H, *H6′*/bipy). $^{31}P\{^1H\}$ NMR ($CDCl_3$): [δ] 49.0 (s, *P*Ph$_3$). Anal. Calc. for $C_{56}H_{42}N_2O_3BrP_2MnRu$ (1088.82): C, 61.77; H, 3.89; N, 2.57. Found: C, 61.46; H, 3.93; N, 2.57%.

4.9. Synthesis of [(η^5-C_5H_5)(dppf)Ru–C≡C–bipy[Mn(CO)$_3$Br] (**14b**)

Complex **14b** was synthesized as described earlier for **14a**, except that **1b** was used instead of **1a**. Experimental details: $Mn(CO)_5Br$ (**13**) (25 mg, 0.091 mmol), **4b** (75 mg, 0.083 mmol). Yield: 55 mg (0.045 mmol, 54% based on **4b**).

M.p.: >218 °C (decomp.). IR (KBr, cm^{-1}): 2040s ($\nu_{C\equiv C}$), 2019s 1929s 1912s (ν_{CO}). ^1H NMR ($CDCl_3$): [δ] 4.05 (br s, 2H, C_5H_4), 4.30 (br s, 2H, C_5H_4), 4.35 (br s, 2H, C_5H_4), 4.38 (s, 5H, C_5H_5), 5.13 (br s, 2H, C_5H_4), 7.26–7.60 (m, 19H, C_6H_5 + bipy), 7.73–7.87 (m, 6H, C_6H_5 + bipy), 8.96 (br s, 1H, *H6*/bipy), 9.18 (br s, 1H, *H6′*/bipy). $^{31}P\{^1H\}$ NMR ($CDCl_3$): [δ] 53.9 (s, *P*Ph$_2$). Anal. Calc. for $C_{54}H_{40}N_2O_3BrP_2MnRu$ (1118.63): C, 57.98; H, 3.60; N, 2.50. Found: C, 57.93; H, 3.84; N, 2.40%.

4.10. Synthesis of [(η^5-C_5H_5)(PPh_3)$_2$Ru–C≡C–bipy{[Ti](μ–σ,π-C≡CSiMe$_3$)$_2$}Cu]BF_4 (**17a**)

[{[Ti](μ–σ,π-C≡CSiMe$_3$)$_2$}Cu(N≡CMe)]BF_4 (**15b**) (85 mg, 0.12 mmol) was dissolved in 30 mL of tetrahydrofuran and **4a** (100 mg, 0.115 mmol) was added in a single portion. After 3 h of stirring at 25 °C the color of the reaction solution was red. The solution was filtered through a pad of Celite and all volatiles were removed in oil-pump vacuum. The remaining red solid was washed twice with 15 mL portions of *n*-hexane and was afterwards dried in oil-pump vacuum. Yield: 140 mg (0.091 mmol, 76% based on **15b**).

M.p.: >185 °C (decomp.). IR (KBr, cm^{-1}): 2044s ($\nu_{RuC\equiv C}$), 1923w ($\nu_{TiC\equiv C}$). ^1H NMR ($CDCl_3$): [δ] −0.46 (s, 18H, Si*Me*$_3$), 0.22 (s, 9H, Si*Me*$_3$), 0.29 (s, 9H, Si*Me*$_3$), 4.37 (s, 5H, C_5H_5), 6.21 (br s, 4H, C_5H_4), 6.26 (br s, 4H, C_5H_4), 7.04–7.25 (m, 18H, C_6H_5), 7.35–7.45 (m, 12H, C_6H_5), 7.50 (dd, $^3J_{H4H3} = 8.5$ Hz, $^4J_{H4H6} = 2$ Hz, 1H, *H4*/bipy), 7.56 (dd, $^3J_{H5'H4'} = 7.5$ Hz, $^3J_{H5'H6'} = 5$ Hz, 1H, *H5′*/bipy), 8.10–8.21 (m, 3H, *H3*,*H4′*,*H6*/bipy), 8.39 (d, $^3J_{H3'H4'} = 8$ Hz, 1H, *H3′*/bipy), 8.44 (d, $^3J_{H6'H5'} = 5$ Hz, 1H, *H6′*/bipy). $^{31}P\{^1H\}$ NMR ($CDCl_3$): [δ] 49.0 (s, *P*Ph$_3$). $^{11}B\{^1H\}$ NMR ($CDCl_3$): [δ] 2.4 (*B*F$_4$). Anal. Calc. for $C_{79}H_{86}N_2P_2BF_4Si_4CuRuTi$ (1537.14): C, 61.73; H, 5.64; N, 1.82. Found: 61.42; H, 5.77; N, 1.64%.

4.11. Synthesis of [(η^5-C_5H_5)(dppf)Ru–C≡C–bipy{[Ti](μ–σ,π-C≡CSiMe$_3$)$_2$}Cu]PF_6 (**17b**)

Experimental conditions and work-up were identical to those for **17a**. Experimental details: [{[Ti](μ–σ, π-C≡CSiMe$_3$)$_2$}Cu(N≡CMe)]PF_6 (**15a**) (55 mg, 0.07 mmol), **4b** (65 mg, 0.07 mmol). Yield: 95 mg (0.058 mmol, 84% based on **15a**).

M.p.: >175 °C (decomp.). IR (KBr, cm^{-1}): 2044s ($\nu_{RuC\equiv C}$), 1924w ($\nu_{TiC\equiv C}$). ^1H NMR ($CDCl_3$): [δ] −0.44 (s, 18H, Si*Me*$_3$), 0.22 (s, 9H, Si*Me*$_3$), 0.29 (s, 9H, Si*Me*$_3$), 4.03 (br s, 2H, C_5H_4/Fc), 4.10 (br s, 2H, C_5H_4/Fc), 4.36 (br s, 2H, C_5H_4/Fc), 4.37 (s, 5H, C_5H_5), 5.02 (br s, 2H, C_5H_4/Fc), 6.17–6.30 (m, 8H, C_5H_4/[Ti]), 7.23–7.59 (m, 17H, C_6H_5 + *H5′*/bipy), 7.63 (dd, $^3J_{H4H3} = 8.5$ Hz, $^4J_{H4H6} = 2$ Hz, 1H, *H4*/bipy), 7.73–7.83 (m, 4H, C_6H_5), 8.12–8.25 (m, 3H, *H3*,*H4′*,*H6*/bipy), 8.38 (d, $^3J_{H3'H4'} = 7.5$ Hz, 1H, *H3′*/bipy), 8.45 (d, $^3J_{H6'H5'} = 4.8$ Hz, 1H, *H6′*/bipy). $^{31}P\{^1H\}$ NMR ($CDCl_3$): [δ] 54.1 (s, *P*Ph$_2$), −145.1 (septet, $^1J_{PF} = 712$ Hz, *P*F$_6$). Anal. Calc. for $C_{77}H_{84}N_2P_3F_6Si_4CuFeRuTi$ (1625.11): C, 56.91; H, 5.21; N, 1.72. Found: C, 56.95; H, 5.61; N, 1.71%.

4.12. Synthesis of [(η^5-C_5H_5)(PPh_3)$_2$Ru–C≡C–bipy{[Ti](μ–σ,π-C≡CSiMe$_3$)$_2$}Ag]ClO_4 (**18a**)

{[Ti](μ–σ,π-C≡CSiMe$_3$)$_2$}$AgOClO_3$ (**16**) (70 mg, 0.098 mmol) was dissolved in 30 mL of tetrahydrofuran

and **4a** (90 mg, 0.104 mmol) was added in a single portion. After 2 h of stirring at 25 °C the color of the reaction solution was red. The solution was filtered through a pad of Celite and all volatiles were removed in oil-pump vacuum. The remaining red solid was washed twice with 15 mL portions of *n*-hexane and was finally dried in oil-pump vacuum. Yield: 115 mg (0.072 mmol, 74% based on **16**).

M.p.: >150 °C (decomp.). IR (KBr, cm^{-1}): 2045s ($\nu_{RuC\equiv C}$), 1955w ($\nu_{TiC\equiv C}$). ^1H NMR ($CDCl_3$): [δ] −0.28 (s, 18H, Si*Me*$_3$), 0.27 (s, 18H, Si*Me*$_3$), 4.37 (s, 5H, C_5H_5), 6.41 (br s, 4H, C_5H_4), 6.46 (br s, 4H, C_5H_4), 7.04–7.25 (m, 18H, C_6H_5), 7.38–7.45 (m, 14H, C_6H_5), 7.46–7.56 (m, 2H, *H4*,*H5′*/bipy), 8.01–8.13 (m, 2H, *H3*,*H4′*/bipy), 8.19–8.27 (m, 2H, *H3′*,*H6*/bipy), 8.53 (d, $^3J_{H6'H5'} = 4.5$ Hz, 1H, *H6′*/bipy). $^{31}P\{^1H\}$ NMR ($CDCl_3$): [δ] 49.1 (s, *P*Ph$_3$). Anal. Calc. for $C_{79}H_{86}O_4N_2P_2ClSi_4AgRuTi$ (1594.12): C, 59.52; H, 5.44; N, 1.76. Found: C, 59.33; H, 5.81; N, 1.67%.

4.13. Synthesis of [(η^5-C_5H_5)(dppf)Ru–C≡C–bipy{[Ti](μ–σ,π-C≡CSiMe$_3$)$_2$}Ag]ClO$_4$ (**18b**)

Experimental conditions and work-up were identical to those for **18a**. Experimental details: {[Ti](μ–σ,π-C≡CSiMe$_3$)$_2$}AgOClO$_3$ (**16**) (45 mg, 0.063 mmol), **4b** (60 mg, 0.067 mmol). Yield: 80 mg (0.049 mmol, 78% based on **16**).

M.p.: >153 °C (decomp.). IR (KBr, cm^{-1}): 2043s ($\nu_{RuC\equiv C}$), 1954w ($\nu_{TiC\equiv C}$). ^1H NMR ($CDCl_3$): [δ] −0.27 (s, 18H, Si*Me*$_3$), 0.27 (s, 18H, Si*Me*$_3$), 4.04 (br s, 2H, C_5H_4/Fc), 4.13 (br s, 2H, C_5H_4/Fc), 4.36 (s, 5H, C_5H_5), 4.37 (br s, 2H, C_5H_4/Fc), 5.07 (br s, 2H, C_5H_4/Fc), 6.41–6.48 (m, 8H, C_5H_4/[Ti]), 7.26–7.56 (m, 17H, C_6H_5 + *H5′*/bipy), 7.61 (dd, $^3J_{H4H3} = 8.5$ Hz, $^4J_{H4H6} = 2$ Hz, 1H, *H4*/bipy), 7.74–7.84 (m, 4H, C_6H_5), 8.06–8.14 (m, 2H, *H3*,*H4′*/bipy), 8.23–8.29 (m, 2H, *H3′*,*H6*/bipy), 8.54 (d, $^3J_{H6'H5'} = 4.5$ Hz, 1H, *H6′*/bipy). $^{31}P\{^1H\}$ NMR ($CDCl_3$): [δ] 53.9 (s, *P*Ph$_2$). Anal. Calc. for $C_{77}H_{84}O_4N_2P_2ClSi_4AgFeRuTi$ (1623.9): C, 56.95; H, 5.21; N, 1.73. Found: C, 56.64; H, 5.20; N, 1.73%.

5. X-ray structure determination of 4b, 10b, 12 and 17b

X-ray structure analysis measurements for **4b** and **17b** were performed with a BRUKER SMART CCD 1k diffractometer at 193 K using oil-coated shock-cooled crystals [33]. The crystal data for **10a** and **12** were collected on an Oxford Gemini S diffractomter at 100 K. The structures were solved by direct methods using SHELXS-97 [34] or SIR-92 [35] and refined by full-matrix least-square procedures on F^2 using SHELXL-97 [36]. All non-hydrogen atoms were refined anisotropically. All hydrogen atom positions were refined using a riding model. The figures in parentheses after each calculated value represent the standard deviation in units of the last significant digit(s).

6. Supplementary material

CCDC 655114, 655116, 659169 and 655115 contain the supplementary crystallographic data for **4b**, **10b**, **12** and **17b**. These data can be obtained free of charge from The Cambridge Crystallographic Data Centre via www.ccdc.cam.ac.uk/data_request/cif.

Acknowledgements

We are grateful to the Deutsche Forschungsgemeinschaft (DFG) and the Fonds der Chemischen Industrie (FCI) for financial support.

References

[1] For example see (a) V. Balzani, A. Juris, M. Venturi, S. Campagna, S. Serroni, Chem. Rev. 96 (1996) 759;
(b) V. Balzani, S. Campagna, G. Denti, A. Juris, S. Serroni, M. Venturi, Acc. Chem. Res. 31 (1998) 26;
(c) C.E. Powell, M.G. Humphrey, Coord. Chem. Rev. 248 (2004) 725;
(d) N.J. Long, C.K. Williams, Angew. Chem., Int. Ed. 42 (2003) 2586;
(e) F. Paul, C. Lapinte, Coord. Chem. Rev. 178–180 (1998) 431;
(f) A. Ceccon, S. Santi, L. Orian, A. Bisello, Coord. Chem. Rev. 248 (2004) 683;
(g) K.M.C. Wong, S.C.F. Lam, C.C. Ko, N. Zhu, V.W.W. Yam, S. Roué, C. Lapinte, S. Fathallah, K. Costuas, S. Kahlal, J.F. Halet, Inorg. Chem. 42 (2003) 7086;
(h) P.J. Low, R.L. Roberts, R.L. Cordiner, F.J. Hartl, Solid State Electrochem. 9 (2005) 717;
(i) S. Back, W. Frosch, I. del Rio, G. van Koten, H. Lang, Inorg. Chem. Commun. 2 (1999) 584;
(j) R. Packheiser, H. Lang, Inorg. Chem. Commun. 10 (2007) 580;
(k) S. Szafert, J.A. Gladysz, Chem. Rev. 106 (2006) PR1–PR33;
(l) M.I. Bruce, P.A. Humphrey, M. Jevric, G.J. Perkins, B.W. Skelton, A.H. White, J. Organomet. Chem. 692 (2007) 1748;
(m) N.J. Long, A.J. Martin, A.J.P. White, D.J. Williams, M. Fontani, F. Laschi, P. Zanello, J. Chem. Soc., Dalton Trans. (2000) 3387;
(n) G. Vives, A. Carella, J.P. Launay, G. Rapenne, Chem. Commun. (2006) 2283.

[2] (a) J. Michl, F. Magnera, Proc. Natl. Acad. Sci. USA 99 (2002) 4788;
(b) M. Levin, P. Kaszynski, J. Michl, Chem. Rev. 100 (2000) 169;
(c) P. Kaszynski, J. Michl, J. Am. Chem. Soc. 110 (1988) 5225.

[3] (a) J.F. Stoddart, Chem. Soc. Rev. 21 (1992) 215;
(b) F.M. Rayoma, J.F. Stoddart, Chem. Rev. 100 (1999) 1643;
(c) V.G. Kessler, Chem. Commun. (2003) 1213;
(d) J.F. Stoddart, Chem. Ber. 124 (1988) 1203.

[4] (a) A.J. Hodge, S.L. Ingham, A.K. Kakkar, M.S. Khan, J. Lewis, N.J. Long, D.G. Parker, P.R. Raithby, J. Organomet. Chem. 488 (1995) 205;
(b) M.I. Bruce, P.J. Low, F. Hartl, P.A. Humphrey, F. de Montigny, M. Jevric, C. Lapinte, G.J. Perkins, R.L. Roberts, B.W. Skelton, A.H. White, Organometallics 24 (2005) 5241;
(c) C.E. Powell, M.P. Cifuentes, A.M. McDonagh, S.K. Hurst, N.T. Lucas, C.D. Delfs, R. Stranger, M.G. Humphrey, S. Houbrechts, I. Asselberghs, A. Persoons, D.C.R. Hockless, Inorg. Chim. Acta 352 (2003) 9;
(d) M. Sato, H. Shintate, Y. Kawata, M. Sekino, M. Katada, S. Kawata, Organometallics 13 (1994) 1956;
(e) F. Paul, B.G. Ellis, M.I. Bruce, L. Toupet, T. Roisnel, K. Costuas, J.-F. Halet, C. Lapinte, Organometallics 25 (2006) 649;

(f) M. Sato, Y. Kawata, H. Shintate, Y. Habata, S. Akabori, K. Unoura, Organometallics 16 (1997) 1693;
(g) D. Touchard, C. Morice, V. Cadierno, P. Haquette, L. Toupet, P.H. Dixneuf, J. Chem. Soc., Chem. Commun. (1994) 859;
(h) D. Touchard, P. Haquette, S. Guesmi, L. Le Pichon, A. Daridor, L. Touplet, P.H. Dixneuf, Organometallics 16 (1997) 3640;
(i) M.I. Bruce, G.A. Koutsantonis, Aust. J. Chem. 44 (1991) 207;
(j) M.G. Humphrey, I.R. Whittall, Organometallics 15 (1996) 1935.
[5] I.Y. Wu, J.T. Lin, J. Luo, S.S. Sun, C.S. Li, K.J. Lin, C. Tsai, C.C. Hsu, J.L. Lin, Organometallics 16 (1997) 2038.
[6] R.D.A. Hudson, J. Organomet. Chem. 637–639 (2001) 47.
[7] (a) S. Köcher, M. Lutz, A.L. Spek, R. Prasad, G.P.M. van Klink, G. van Koten, H. Lang, Inorg. Chim. Acta 359 (2006) 4454;
(b) S. Köcher, G.P.M. van Klink, G. van Koten, H. Lang, J. Organomet. Chem. 684 (2003) 230.
[8] R.A.T.M. Abbenhuis, I. del Río, M.M. Bergshoef, J. Boersma, N. Veldman, A.L. Spek, G. van Koten, Inorg. Chem. 37 (1998) 1749.
[9] (a) G.J. Stor, S.L. Morrison, D.J. Stufkens, A. Oskam, Organometallics 13 (1994) 2641;
(b) W.A. Herrmann, W.R. Thiel, J.G. Kuchler, Chem. Ber. 123 (1990) 1953;
(c) L.H. Staal, A. Oskam, K. Vrieze, J. Organomet. Chem. 170 (1979) 235.
[10] (a) S. Back, R.A. Gossage, H. Lang, G. van Koten, Eur. J. Inorg. Chem. (2000) 1457;
(b) S. Back, R.A. Gossage, M. Lutz, I. del Río, A.L. Spek, H. Lang, G. van Koten, Organometallics 19 (2000) 3296;
(c) S. Back, M. Albrecht, A.L. Spek, G. Rheinwald, H. Lang, G. van Koten, Organometallics 20 (2001) 1024;
(d) S.L. James, G. Verspui, A.L. Spek, G. van Koten, Chem. Commun. (1996) 1309.
[11] R. Packheiser, B. Walfort, H. Lang, Organometallics 25 (2006) 4579.
[12] I. del Rio, S. Back, M.S. Hannu, G. Rheinwald, H. Lang, G. van Koten, Inorg. Chim. Acta 300–302 (2000) 1094.
[13] (a) L.-B. Gao, L.-Y. Zhang, L.-X. Shi, Z.-N. Chen, Organometallics 24 (2005) 1678;
(b) M. Sato, M. Sekino, J. Organomet. Chem. 444 (1993) 185.
[14] R. Packheiser, A. Jakob, P. Zoufala, B. Walfort, H. Lang, Organometallics (in press).
[15] For example see (a) P. Debroy, S. Roy, Coord. Chem. Rev. 251 (2007) 203, and refs. cited therein;
(b) J.T. Lin, S.S. Sun, J.J. Wu, L. Lee, K.J. Lin, Y.F. Huang, Inorg. Chem. 34 (1995) 2323;
(c) B. Bildstein, Coord. Chem. Rev. 206–207 (2000) 369;
(d) S. Le Stang, F. Paul, C. Lapinte, Organometallics 19 (2000) 1035.
[16] (a) M. Albrecht, G. van Koten, Angew. Chem., Int. Ed. Engl. 40 (2001) 3750;
(b) P. Steenwinkel, R.A. Gossage, G. van Koten, Chem. Eur. J. 4 (1998) 759;
(c) R.A. Gossage, L.A. van de Kuil, G. van Koten, Acc. Chem. Res. 31 (1998) 423.
[17] (a) I. del Río, S. Back, M.S. Hannu, G. Rheinwald, H. Lang, G. van Koten, Inorg. Chim. Acta 300–302 (2000) 1094;
(b) S. Back, G. Rheinwald, I. del Río, G. van Koten, H. Lang, Acta Cryst. Sect. E 57 (2001) 444;
(c) T.W. Welch, S.A. Ciftan, P.S. White, H. Holden Thorp, Inorg. Chem. 36 (1997) 4812;
(d) I. del Río, R.A. Gossage, M. Lutz, A.L. Spek, G. van Koten, J. Organomet. Chem. 583 (1999) 69.
[18] (a) B.J. Coe, T.J. Meyer, P.S. White, Inorg. Chem. 34 (1995) 593;
(b) J.L. Templeton, J. Am. Chem. Soc. 101 (1979) 4906;
(c) P.S. Moritz, A.A. Diamantis, R.F. Keene, M.R. Snow, E.R.T. Tiekink, Aust. J. Chem. 41 (1988) 1353.
[19] (a) H. Lang, D.S.A. George, G. Rheinwald, Coord. Chem. Rev. 206–207 (2000) 101;
(b) H. Lang, G. Rheinwald, J. Prakt. Chem. 341 (1999) 1;
(c) H. Lang, K. Köhler, S. Blau, Coord. Chem. Rev. 143 (1995) 113.
[20] T. Luczak, M. Beltowska-Brzezinska, M. Bron, R. Holze, Vib. Spectrosc. 15 (1997) 17.
[21] S. Back, R.A. Gossage, G. Rheinwald, I. del Río, H. Lang, G. van Koten, J. Organomet. Chem. 582 (1999) 126.
[22] (a) M.I. Bruce, P.J. Low, K. Costuas, J.-F. Halet, S.P. Best, G.A. Heath, J. Am. Chem. Soc. 122 (2000) 1949;
(b) M.I. Bruce, B.C. Hall, B.D. Kelly, P.J. Low, B.W. Skelton, A.H. White, J. Chem. Soc., Dalton Trans. (1999) 3719;
(c) M.I. Bruce, B.G. Ellis, P.J. Low, B.W. Skelton, A.H. White, Organometallics 22 (2003) 3184.
[23] Ferrocene/ferrocenium redox couple G. Gritzner, J. Kuta, Pure Appl. Chem. 56 (1984) 461.
[24] A conversion of given electrode potentials to the standard normal hydrogen electrode is possible H. Strehlow, W. Knoche, H. Schneider, Ber. Bunsenges. Phys. Chem. 77 (1973) 760.
[25] H.E. Gottlieb, V. Kotlyar, A. Nudelman, J. Org. Chem. 62 (1997) 7512.
[26] (a) F.L. Joslin, J.T. Mague, D.M. Roundhill, Organometallics 10 (1991) 521;
(b) M.I. Bruce, N.J. Windsor, Aust. J. Chem. 30 (1977) 1601.
[27] (a) X.L. Lu, J.J. Vittal, E.R.T. Tiekink, G.K. Tan, S.L. Kuan, L.Y. Goh, T.S.A. Hor, J. Organomet. Chem. 689 (2004) 1978;
(b) M.I. Bruce, I.R. Butler, W.R. Cullen, G.A. Koustanonis, M.R. Snow, E.R.T. Tieknik, Aust. J. Chem. 41 (1988) 963.
[28] (a) V. Grosshenny, F.M. Romero, R. Ziessel, J. Org. Chem. 62 (1997) 1491;
(b) P.F.H. Schwab, F. Fleischer, J. Michl, J. Org. Chem. 67 (2002) 443;
(c) J. Polin, E. Schmohel, V. Balzani, Synthesis 3 (1998) 321.
[29] (a) M. Janka, G.K. Anderson, N. Rath, Organometallics 23 (2004) 4382;
(b) L. Yu, J.S. Lindsey, J. Org. Chem. 66 (2001) 7402;
(c) B.T. Holmes, W.T. Pennington, T.W. Hanks, Synth. Commun. 33 (2003) 2447.
[30] K.J. Reimer, A. Shaver, Inorg. Synth. 28 (1990) 154.
[31] M.D. Janssen, M. Herres, L. Zsolnai, A.L. Spek, D.M. Grove, H. Lang, G. van Koten, Inorg. Chem. 35 (1996) 2476.
[32] H. Lang, M. Herres, L. Zsolnai, Organometallics 12 (1993) 5008.
[33] (a) T. Kottke, D. Stalke, J. Appl. Crystallogr. 26 (1993) 615;
(b) T. Kottke, R.J. Lagow, D. Stalke, J. Appl. Crystallogr. 29 (1996) 465;
(c) D. Stalke, Chem. Soc. Rev. 27 (1998) 171.
[34] G.M. Sheldrick, Acta Crystallogr., Sect. A 46 (1990) 467.
[35] A. Altomare, G. Cascarano, C. Giacovazzo, A. Gualardi, J. Appl. Cryst. 26 (1993) 343.
[36] G.M. Sheldrick, SHELXL-97, Program for Crystal Structure Refinement, University of Göttingen, 1997.